Generalized Process Model for

Solid Sorbent Direct Air Capture Contactors

by

Kshitij Mukeshbhai Patel

A Thesis Presented in Partial Fulfillment
of the Requirements for the Degree of
Master of Science

Approved October 2023 by the
Graduate Supervisory Committee:

Matthew Green, Chair
Klaus Lackner
John Cirucci

ARIZONA STATE UNIVERSITY

December 2023

ABSTRACT

Global emissions of carbon dioxide are reaching new heights every year since the Industrial Revolution. A major contributor to this is fossil fuel consumption. The consumption trend has indicated all this. It has also strengthened the argument for the need to cut down emissions and sweep out historical emissions through the implementation of Carbon Capture, Utilization, and Storage (CCUS) and Carbon Dioxide Removal (CDR) technologies respectively. This is required to control global warming. Direct Air Capture (DAC) is one of the CDR technologies. Extensive research and projections have suggested that DAC has tremendous potential to achieve global climate change mitigation goals. The feasibility of DAC is proven but work is required to bridge gaps in DAC research to make it affordable and scalable. Process modelling is an approach used to address these concerns. Current DAC research in system design and modelling is discrete and existing models have limited use cases. This work is focused on the development of a generalized process mass transfer model for the capture stage of solid sorbent DAC contactors. It provides flexibility for defining contactor geometry, selection of ambient conditions, and versatility to plug different sorbents in it for CO_2 capture. The modelling procedure is explained, and a robustness check is performed to ensure model integrity. The results of the robustness check and sensitivity analysis are then explained. This research is part of a long-term effort to create a complete modelling package for the DAC community to boost research and development to large-scale deployments.

DEDICATION

I dedicate this thesis to my parents: Mr. Mukesh Patel and Mrs. Bharati Patel, whose immense love, support, and guidance molded me into the person I am today. Your stories of struggle and handwork have always inspired me to never let myself down even in the hardest circumstances. You always believed in me even when I was not certain. Your calmness and composure taught me to keep patience and keep working towards the set goal. We were apart on different continents, but I never felt alone because your frequent check-ins and talks always soothed me and gave me the required confidence. Thank you for everything.

ACKNOWLEDGEMENTS

I would like to express my gratitude to the following individuals and organizations for their constant guidance and invaluable contribution to the completion of this thesis. Firstly, I would like to thank my thesis advisor Dr. Matthew Green for allowing me to do this research under his supervision and suggesting this novel topic. I am beholden to his immense support and guidance throughout this time. I want to extend my sincere gratitude to my committee members Dr. Klaus Lackner and John Cirucci. They directed me whenever I went off track and gave me some critical insights that were crucial for taking important decisions which has improved the quality of my thesis considerably. I am very grateful to Travis Johnson and the Center for Negative Carbon Emissions for providing me with this opportunity and giving me financial support and resources. My sincere appreciation is to Adam Berger and Joesph Swisher from the Electric Power Research Institute who shared some valuable insights on several critical topics related to the thesis. Last but certainly not least, I am thankful to Arizona State University, Tempe campus who made my dream of pursuing a master's come true.

TABLE OF CONTENTS

Page

LIST OF TABLES……..vi

LIST OF FIGURES…….……..vii

LIST OF SYMBOLS…….…….ix

LIST OF ACRONYMS……..xi

CHAPTER

1. INTRODUCTION……...1

    Overview of CDR Technologies...……...3

    Introduction to Direct Air Capture…….……..4

    Process Modelling in DAC (Literature Review) …….……...7

2. GENERALIZED PROCESS MODEL……9

    Assumptions……..10

3. MODELLING APPROACH……..…...11

4. FLOW OF INFORMATION IN THE MODEL……13

    Enter Process Parameters……...14

    Calculations of Secondary Process Parameters...……..15

    Mass Transfer Calculations..……..……15

    Mass Balance……...……..18

    Formulating Results...……..……..19

    Data Visualization……..19

    Final Report Creation…..…….....22

CHAPTER Page

5. ROBUSTNESS CHECK AND SENSITIVITY ANALYSIS……24

Effect of Ambient Temperature Change..……..25

Effect of Ambient Pressure Change……...……27

Effect of Channel Velocity Change……...…….30

Effect of Channel Thickness Change……..……...30

Effect of Channel Height Change……..……31

Effect of Regeneration Temperature……..……34

6. CONCLUSION…….…….38

7. FUTURE DIRECTIONS……...41

REFERENCES……..42

APPENDIX

A. PYTHON CODE: GENERALIZED PROCESS MODEL FOR SOLID SORBENT DIRECT AIR CAPTURE CONTACTORS…….……48

B. SAMPLE DESIGN RESULT REPORT……..78

LIST OF TABLES

Table Page

1. Classification of Prevailing DAC Technologies……..……...5
2. Required Inputs for the Generalized DAC Model……...……..14
3. Robustness Check Highlights Table…….…….24
4. The Effect of Temperature on Equilibrium Loading…….…….27
5. The Effect of Pressure on Equilibrium Loading…….……...28
6. Effect of Velocity on Reynold's Number and Interphase MT Coefficient…….31
7. Effect of channel thickness of the contactor on the daily capture capacity……...33
8. The Effect of Regeneration Temperature on the Initial Loading of the Sorbent Material…….….36
9. Performance Estimation from The Model Based on Obtained Cycle Time and Loading Capacity…….……..37

LIST OF FIGURES

Figure Page

1. Global Energy Trend (Data Source: EI Statistical Review of Energy) ……..…1
2. Energy-Related CO_2 Emissions (Data Source: EI Statistical Review of Energy)..2
3. Some of The Currently used Popular Geometries for DAC Contactors…….9
4. Sample Diagram Showcasing the Creation of Finite Elements……12
5. Sequential Finite Elements from Different Directions……..12
6. Steps Involved in Generalized Process Modelling for Solid Sorbent DAC Contactors…...……...13
7. Unit Cell Loading Curves…..……20
8. Total Channel Loading Curve…….……...21
9. Average Loading Rate Curve…….……21
10. Breakthrough Curve at Different Loading Levels (25%, 50%, 75%, and 90% of Net Loading) …….22
11. The Effect of Ambient Temperature on Channel Loading. For 273K, 290K, and 298K Regeneration Conditions Are 368K And 3000 Pa While For 330K It Is 373K and 1000 Pa……...……...25
12. The Effect of Ambient Temperature on Loading Rate, For 273K, 290K, 298K, 300K, and 373K...…….…….……25
13. The Effect of Pressure on Total Channel Loading At 298K..…….…...28
14. The Effect of Pressure on The Loading Rate At 298K….……..…29
15. The Effect of Velocity on Channel Loading At 98000 Pa and 298K…...…….….29

Figure Page

16. The Effect of Velocity on The Average Driving Force at 98000 Pa and 298K.....30

17. The Effect of Channel Thickness at 98000 Pa and 298K…….…….32

18. The Effect of Channel Thickness on the Average Loading Rate at 98000 Pa And 298K…….……..32

19. The Effect of Channel Height on Loading Rate at 98000 Pa and 298K……33

20. The Effect of Channel Height on Driving Force at 98000 Pa and 298K…….…..34

21. The Effect of Regeneration Temperature at 98000 Pa and 298K…….….35

22. The Change in the Average Driving Force for CO_2 with Regeneration Temperature at 98000 Pa and 298K……...……36

23. The Performance of the DAC Contactor Channel at Different Locations…….39

LIST OF SYMBOLS

1. A – Cross Section Area of Mass Transfer (M^2)
2. C_{CO2} – CO_2 Concentration in the Atmosphere (Ppm)
3. D_{bed} – Diffusivity of CO_2 in the Bed Pores (Interparticle) (M^2/S)
4. D_{CO2} – Diffusivity of CO_2 in Air (M^2/S)
5. $D_{particle}$ – Diffusivity of CO_2 in the Particle Pores (Intraparticle) (M^2/S)
6. $D_{particle}$ – Particle Diameter (M)
7. D_{pore} – Average Pore Diameter (M)
8. Λ – Mean Free Path (M)
9. D_K – Knudsen Diffusion Coefficient (M^2/S)
10. F_{air} – Volumetric Air Flowrate (M^3/S)
11. H – Gap Between Two Beds (M)
12. K – Overall Mass Transfer Coefficient
13. $K_{interphase}$ – Interphase Mass Transfer Coefficient (M/S)
14. L – Depth of the Bed (M)
15. Mw_{air} – Molar Mass of Air (G/Mol)
16. N_{re} – Reynold's Number
17. N_{sc} – Schmidt Number
18. P – Pressure (Pa)
19. Q_{CO2} – CO_2 Loading at a Given Pressure (Mmol/G)
20. S – Thickness of the Bed (M)
21. Sh – Sherwood Number

22. T – Bed Loading Time (S)

23. T – Temperature (K)

24. V – Wind Velocity (M/S)

25. W – Width of the Bed (M)

26. E_{bed} – Porosity of the Bed

27. $E_{particle}$ – Porosity of the Particle

28. M – Viscosity of Air (Pa S)

29. P_{bed} – Bed Density (Kg/M^3)

30. $P_{sorbent}$ – Sorbent Density (Kg/M^3)

31. T_{bed} – Tortuosity of the Bed

32. $T_{particle}$ – Tortuosity of the Particle

LIST OF ACRONYMS

1. AI – Artificial Intelligence
2. BP – British Petroleum
3. CCS – Carbon Capture and Storage
4. CCUS – Carbon Capture, Storage and Utilization
5. CDR – Carbon Dioxide Removal
6. CO_2 – Carbon Dioxide
7. DAC – Direct Air Capture
8. DAC-DT – Direct Air Capture Digital Twin
9. EI – Energy Institute
10. GHG – Green House Gas
11. GT – Global Thermostat
12. H_2O - Water
13. IPCC – Intragovernmental Panel on Climate Change
14. LCA – Life Cycle Analysis
15. MT – Mass Transfer
16. NOAA – National Oceanic and Atmospheric Administration

CHAPTER 1

INTRODUCTION

The world has seen a significant rise in greenhouse gas (GHG) emissions since the Industrial Revolution. As per IPCC's AR5 report, Carbon dioxide (CO_2) is a major contributor to this global warming with ~75% of total GHG emissions since 1970 [1]. Then in 2023, IPCC's AR6 synthesis report clearly indicated the requirement of negative emissions technologies to clean up past anthropogenic emissions [2]. This means Carbon Dioxide Removal (CDR) technologies are required to develop and deploy at a scale to achieve our climate goal of restraining the global temperature rise to 1.5 °C or 2 °C.

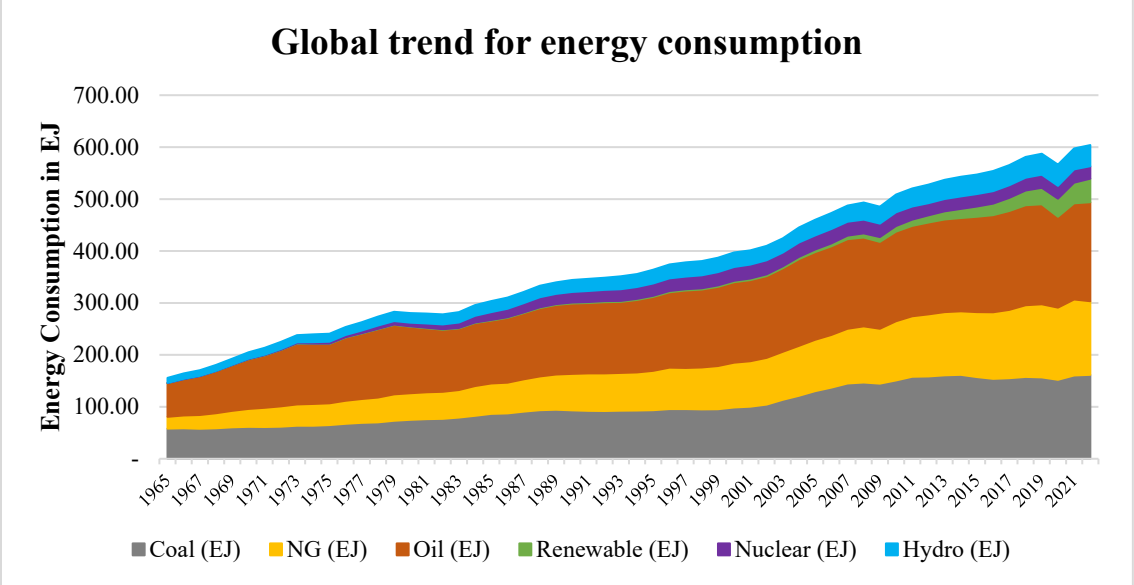

Figure 1. Global energy trend (Data Source: EI Statistical Review of energy)

This can be understood better with some real data. Figure 1 shows the global energy consumption since 1965. The data is taken from the Energy Institute's Statistical Review

of World Energy (formerly by BP) [3]. It clearly indicates that the global energy demand is increasing steadily and the contribution of fossil fuel in meeting that demand is still >80% as per the 100% stacked bar graph (yellow color) in Figure 2. Rising energy consumption and the domination of carbon-intensive fuels are leading to emitting more CO_2 as shown by the red line in Figure 2. This indicates that the pace of the current global energy transition to renewables is not sufficient, and the forward path will not be easy. It will require Carbon Capture, Storage, and Utilization (CCUS) to reduce emissions and Carbon Dioxide Removal (CDR) techniques to clean up historical emissions. The forward discussion will be focused on CDR technologies.

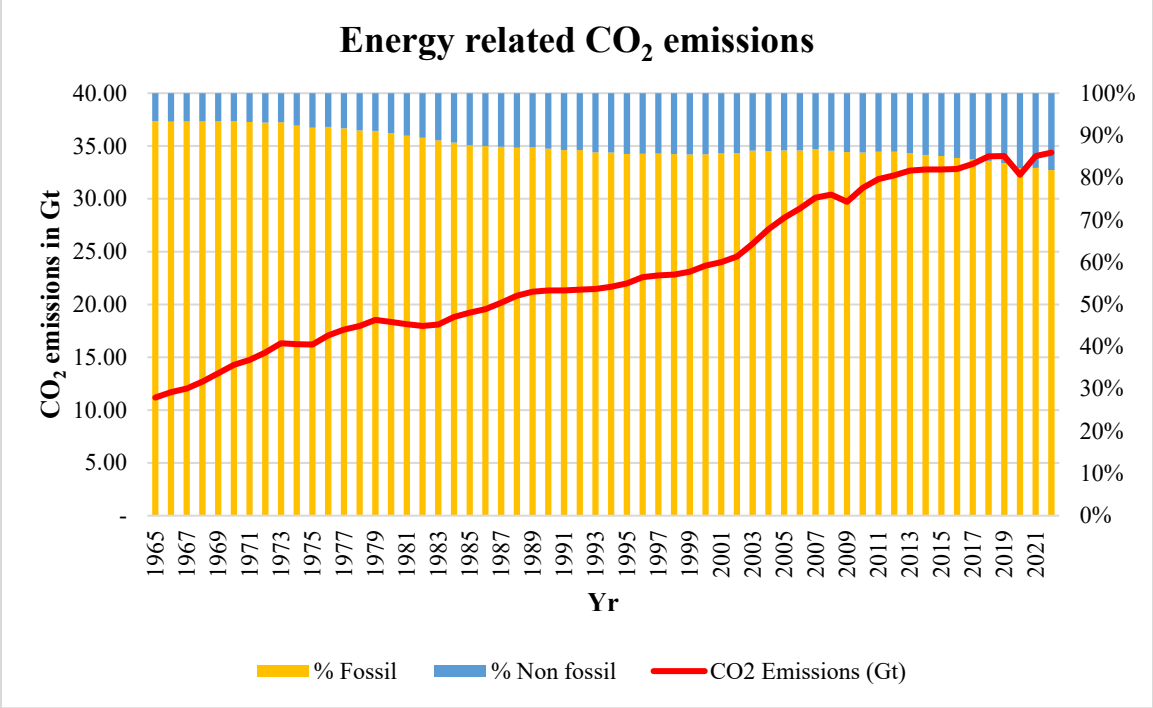

Figure 2. Energy-related CO_2 emissions (Data Source: EI Statistical Review of Energy)

Overview of CDR Technologies:

There are different CDR approaches evaluated by the IPCC [4]. Each of these has different fundamentals to capture and sequester carbon for varying time periods. The most well-known approach is forestation: reforestation and afforestation [5]. Soil carbon sequestration or carbon farming is another approach where different soil management tactics are used to capture and store more carbon in the land [6]. Biochar is a carbon-rich solid material obtained by the partial combustion of biomass in an oxygen-lean environment whose composition varies based on pyrolysis conditions. A good quality biochar usually has >65% C in it [7, 8]. Peatland covers 3% of the global land area which also has potential for CDR via restoration [9]. The carbon captured by ocean and coastal ecosystems is known as blue carbon [10].

Artificial ocean upwelling is another approach where deep sea water is moved to the ocean surface [11]. Ocean iron fertilization is an artificial CDR process in which iron is added to the ocean [12]. Both abovementioned CDR technologies can stimulate the growth of phytoplankton that can absorb CO_2 and store carbon after their death. In ocean alkalinization, alkaline substances are added to the water which can increase the carbon storage capacity of the ocean [13]. Enhanced weathering is an on-shore CDR process that utilizes finely grounded earth materials like silicate rocks that have an affinity to bind CO_2 [14]. Bioenergy with carbon capture and storage (BECCS) converts biomass into energy and captures the CO_2 generated during the process which is then sequestered

permanently [15]. Direct Air Capture (DAC) is also one of the CDR approaches that capture CO_2 directly from the air which is where further attention will be directed.

Introduction to Direct Air Capture:

The concept of DAC was given by Dr. Klaus Lackner in 1999 and since then, it has developed considerably. The comparison given in the IPCC's AR6 report indicates that DAC has great potential with the least trade-offs compared to other CDR techniques to meet the set targets of emission reduction [4]. The classification of current DAC technologies can be done in two ways. One is by the type of mass transfer phenomena used: adsorption-based (solid) and absorption-based (liquid). The second method of classification is based on the flow of air: passive systems and forced systems. Table 1 gives a fair idea about this classification for prevailing DAC technologies. There are several other technologies based on biotechnology [16, 17] that are not considered here because of their nascency. From this, it can be said that the solid sorbent DAC is currently dominating the field. The reason is the simplicity of the design, lower regeneration cost, and ease of operation [18].

Once CO_2 is captured from the air, the material needs to be regenerated to separate out CO_2. This is where energy input is required in addition to the fan power if the system is forced circulation. Different approaches are being tested and implemented for this. E.g., thermal swing, pressure swing, and a combination of these [19, 20, 21, 22]. Novel approaches like autothermal, moisture swing, pH swing, etc. are also identified and under

investigation at different scales currently [23, 24, 25]. Another observation is that current DAC technologies are batch processes that limit the throughput of the system. Research is progressing for novel concepts like the continuous belt approach and CO_2 membranes, but they are still very nascent and need to be proven [26, 27, 28].

Table 1. Classification of prevailing DAC technologies

Classification 1 ► **Classification 2▼**	Adsorption based technology	Absorption based technology
Passive DAC	Carbon Collect Heirloom Heimdal Parallel Carbon	Carbon Blade
Forced DAC	Climeworks TerraFixing Carbon Reform Susteon Global Thermostat Noya Avnos CarbonCapture Aircapture Removr Soletair Power Blancair ReCarbn Carbyon Octavia Carbon	x/44 Capture6 Repair Carbon Engineering (Now Oxy) Aircela

Pilot-scale deployments showed the world that DAC is feasible. Now the next step is to make DAC more affordable and scalable so that it can be deployed at a scale. Major areas where DAC currently struggles are sorbent development and high energy consumption. Both things are interrelated. The feasibility of DAC was analyzed with materials that

were developed for some other applications. From the recent reviews, it is clear that a fair amount of research is going on for DAC sorbent synthesis, and promising materials are being formulated [29, 30, 31, 32]. Questions that still need answers are around scalability, cheap and efficient synthesis techniques, Life Cycle Analysis (LCA) of the sorbent, and the cost associated with the sorbent production [30]. All these contribute to the capital cost.

In the feasibility studies, the cost is not a major concern. However, for developing a successful and deployable technology, affordability is one of the criteria. This is where DAC faces another barrier. The current energy demand for regeneration is high, for liquids it is 6-10 GJ/t of CO_2, and for solids it is up to 8 GJ/t of CO_2 [33]. This determines the operating costs. The set target for DAC CO_2 capture is <$100 while current estimates are around $ 125-335 /t of CO_2 as per IEA [34]. The performance of DAC is also variable and highly dependent on ambient conditions [35, 36]. This considerably affects the energy requirements and in turn the carbon footprint. Researchers are positive that the cost will go down with time as DAC becomes mature [30, 37]. On the other hand, our climate goals are becoming more stringent which requires early deployment of these technologies.

The modern world is observing a transition towards digitalization, and it has tremendous potential to solve these climate problems by implementing these novel approaches. These technologies can be used to support DAC research and deployment too. The article on the application of Digital Twin in DAC has shown this direction [38]. The use of AI in sorbent development is also gaining traction [39]. But all this digitalization will require a solid

foundation, an understanding of DAC, and models that can replicate real-world operations in digital ecosystems.

Process Modelling in DAC (Literature Review):

Process modelling is a proven approach for solving problems of process design and understanding parameters affecting the system [40]. These models are designed to mimic actual operations with the use of mathematical equations [41]. The groundwork for developing a whole simulation package is set by these process models. As per the DAC Digital Twin article, these models will become pillars of a fully functional DAC Digital Twin and virtual carbon ecosystem [38].

Researchers are using different approaches for process modelling in DAC [19, 20, 21, 22, 41]. According to Marinic et. al. (2023), modelling in DAC can be segregated into three categories: 1) Nanoscale, 2) Mesoscale, and 3) Macroscale [42]. Quantum mechanics is studied with nanoscale modelling. Mesoscale modelling is used to determine the thermodynamic and physical properties of the sorbent material and understand the CO_2 capture mechanism. Macroscale modelling is the most researched area in DAC where transport rates are determined for system design, rating, and simulation. These models and results are often used to formulate a complete unit operation scheme for the determination of the total cost and efficiency of the DAC facility.

After the literature review, it was found that very little work is done on constructing a model from a user perspective [19, 20, 21, 36, 41, 43]. In other words, there is no model formed yet that can provide engineers, researchers, and designers with functionalities in terms of designing various geometries for sorbent material with known isotherm data and testing them in different ambient conditions. Research is done to test these variabilities individually [36, 44, 45]. There is inconsistency since various platforms are used to formulate these models. This obstructs integration and makes it difficult to interpret or anticipate outcomes as all these models are not developed in the same modelling environment.

This work is an effort to bridge the abovementioned gaps in macroscale DAC modelling by the development of a generalized process model. This will let the user define and test various modular form factors for the air contactor that can be scaled easily for deployment. The model will let users set process conditions for DAC, giving them flexibility for testing the designed contactor in different geographical regions to understand variability in performance. Another versatility will come with friendliness to test the sorbent of their choice. In the end, the goal is to develop a comprehensive package for the DAC contactors that can be used to design and test systems virtually before physically building one to predict the performance.

CHAPTER 2

GENERALIZED PROCESS MODEL

The research is an initiation of a long-term effort where current activity is focused on the development of a process model for solid sorbent DAC contactors that can operate in a turbulent flow regime. The model can design and test geometries with sorbents in the form of beads or particles. It can also test geometries with sorbent coating or laminates. This will require minor adjustments in the mass transfer resistances. It is capable of modelling air contactor channels of any circular or non-circular cross-sections. Figure 3 shows some of the popular modular geometries used in solid sorbent DAC contactors where the first one uses particles or beads of sorbents while the other two normally use laminates or coating of the sorbent material. There are several assumptions that need to be made to elucidate the modelling activity. These are stated below.

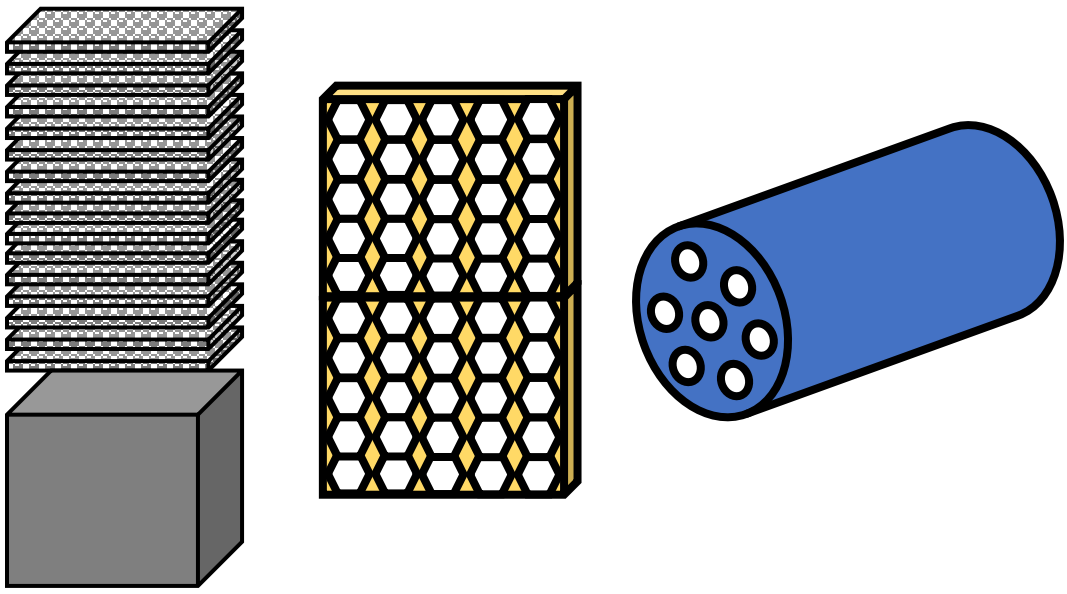

Figure 3. Some of the currently prevailing geometries for DAC contactors

Assumptions:

- The temperature, pressure, and composition of air at the front of the channel will be uniform.
- Ideal gas law is used for the calculation of fluid properties.
- The cross-section of the channel is constant throughout the length.
- No slip condition is followed.
- The sorbent particles or beads are uniformly distributed in the bed.
- The sorbent particles are assumed to be of sphere in shape.
- The series resistance model is used for mass transfer calculations.
- Co-adsorption of H_2O is neglected.
- The turbulent flow of air in the channel makes the concentration of air along the height of the channel uniform over each unit cell.
- Heat associated with adsorption is neglected.

CHAPTER 3

MODELLING APPROACH

Modularity and scalability can complement the deployment of DAC in an efficient way and at a required scale. Most of the prevailing technologies: Climeworks, Heirloom, CarbonCollect, etc. are using this approach by simple replication of the base system. With this, modelling performed for a single unit can be replicated and applied to the whole system or cluster.

Therefore, in this work efforts are made to construct a model that can design and test a modular single channel of any cross section whose replication can lead to easy scale up, to form an efficient air contactor of a defined capacity. The current model development follows a proven approach of finite element discretization as shown in Figure 4. The whole channel is segmented into small defined-size elements and each of these elements are then modelled individually and sequentially as required as shown in Figure 5. In sequential finite elements, outputs from the previous element will become inputs for the next element.

The model is formed in such a way that it has user-defined geometry and process parameters. This gives the model versatility to test combinations of geometry and ambient conditions to help select the most optimum conditions or geometry. It has the flexibility to test any potential sorbent materials with known adsorption isotherm parameters.

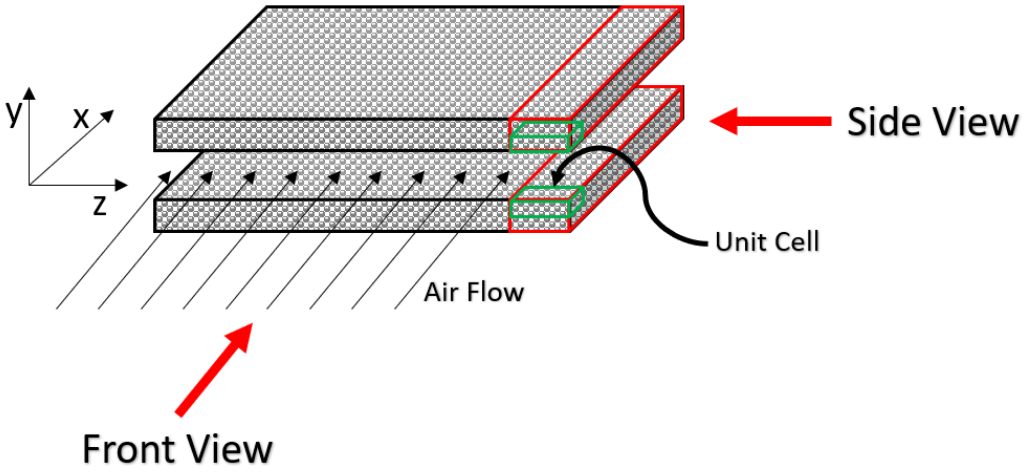

Figure 4. Sample diagram showcasing the creation of finite elements.

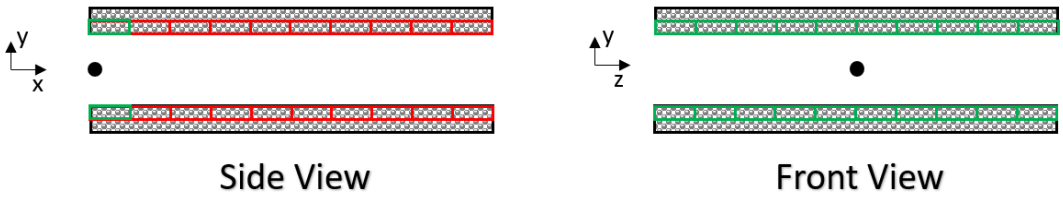

Figure 5. Sequential finite elements from different directions

CHAPTER 4

FLOW OF INFORMATION IN THE MODEL

Figure 6 shows the steps involved in this modelling. It is a seven-step procedure that starts with giving inputs for geometry of the channel, process conditions in which the design needs to be tested, and the sorbent being used. This is followed by the calculation of fluid properties and mass transfer resistances. After this, mass balance is performed for each finite element and iterations are continued until either the model approaches equilibrium or the defined cycle time is reached. The results generated in these iterations are then organized accordingly to generate arrays. These arrays are then used to generate data visualizations i.e., graphs to understand trends. The last step will be the report generation where the model provides the user with a design result sheet in PDF format which consists of design and performance data.

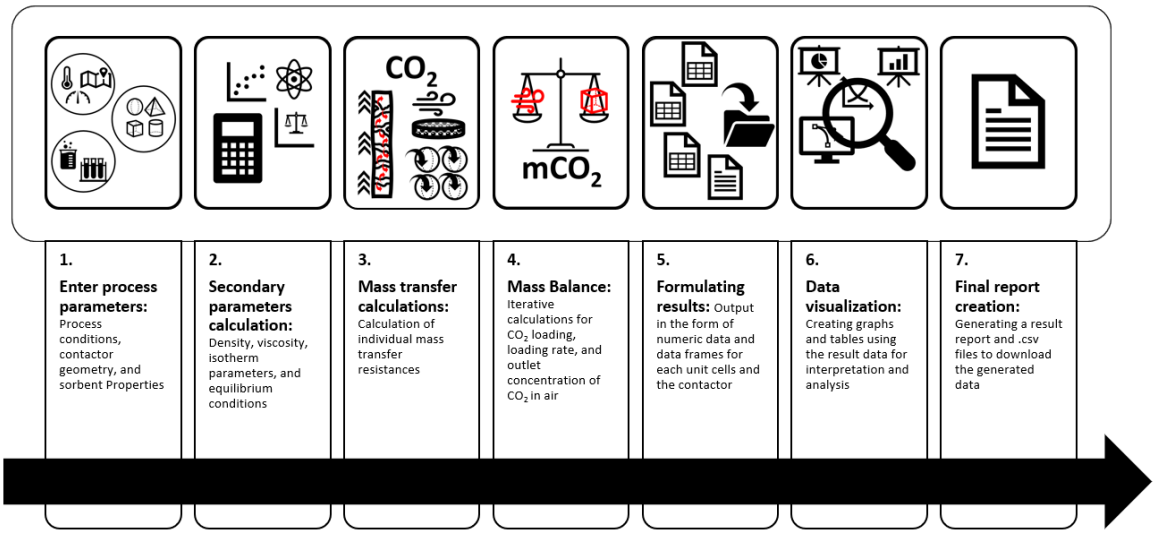

Figure 6. Steps involved in Generalized process modelling for solid sorbent DAC contactors.

Each of these steps will now be explained in detail in the following section.

Enter Process Parameters:

In this step, the model takes input from the user for channel geometry, process conditions, and about the sorbent being used or tested for the case. Table 2 shows all the required inputs for the model. It also gives information about base case that will be used for later comparison. Microsoft Excel is used for taking inputs from the user which are then fed to the model in Python.

Table 2. Input parameters required for this generalized DAC model.

Parameter	Value (Sample inputs)	Unit
Temperature (T)	298	K
Pressure (P)	98000.00	Pa
Velocity in the channel (v)	2.00	m/s
CO_2 level (C-CO2)	420.00	ppm
Length of channel (L)	0.20	m
Width of channel (W)	1.00	m
Thickness of channel wall(S)	0.015	m
Height of the channel (H)	0.03	m
Sorbent type	MOF (MIL-101-Cr)	None
Sorbent Density (ρ-sorbent)	1000.00	kg/m^3
Bed void fraction (ε-bed)	0.40	None
Particle porosity (ε-particle)	0.40	None
Particle diameter (d-particle)	0.000500	m
Isotherm	Toth	None
Average pore diameter	0.000000001	m
Regeneration temperature	368	K
CO_2 partial pressure during Regeneration	3000	Pa

Calculations of Secondary Process Parameters:

The required properties for the fluid (here air), contactor channel, and numbers of finite elements will be calculated in this section using the following equations. Eq. 1 is used for density calculation based-on the assumption of ideal gas law. Sutherland's law is used for the viscosity calculation as shown in eq. 2 [46]. The bed density is calculated by considering interparticle and intraparticle porosity (eq. 3).

$$\rho_{air} = \frac{PMw_{air}}{1000RT} \quad (1)$$

$$\mu_{air} = \frac{C1\ T^{1.5}}{(T + C2)} \quad (2)$$

where C1 = 1.458 X 10^{-6} and C2 = 110.4

$$\rho_{bed} = (1 - \varepsilon_{bed})(1 - \varepsilon_{particle})\, \rho_{sorbent} \quad (3)$$

$$d_{eq} = \frac{4WH}{2W} \quad (4)$$

$$No.\ of\ unit\ cells = \frac{L\ (in\ m)}{Resolution\ factor} \quad (5)$$

Consideration of equivalent diameter is also important for channels with non-circular cross sections (eq. 4). The number of unit cells will be calculated from eq. 5 using the length of the channel.

Mass Transfer Calculations:

The process model is focused on the mass transfer (MT) of CO_2 from air to the sorbent material. The transfer of CO_2 has three resistances: 1) Interphase MT resistance, 2)

Interparticle MT resistance, and 3) Intraparticle MT resistance. All three barriers need to be crossed to get CO_2 adsorbed.

The first resistance will be the interphase MT coefficient which is calculated using the following equations and empirical correlation [47]. Properties required for the calculation of the Reynolds number and Schmidt number are either already defined or are calculated in step 2.

$$N_{Sc} = \frac{\mu_{air}}{\rho_{air} D_{CO2}} \quad (6)$$

$$N_{Re} = \frac{v\, d_{eq}\, \rho_{air}}{\mu_{air}} \quad (7)$$

$$Sh = 0.023 N_{Re}^{0.83} {N_{Sc}}^{0.44} \quad (8)$$

$$Sh = \frac{D_{CO2}\, d_{eq}}{k} \quad (9)$$

The second resistance will be the interparticle MT coefficient. This is important in contactor made with beads or particles. Eq. 10 and 11 are used for identifying this resistance [48].

$$D_{bed} = \frac{\varepsilon_{bed} D_{CO2}}{\tau_{bed}} \quad (10)$$

$$\tau_{bed} = \frac{1}{\varepsilon_{bed}} \quad (11)$$

As per Perry's Chemical Engineers Handbook, for a more realistic design, experimental results of tortuosity (τ_{bed}) should be utilized [50]. Currently, due to the lack of information, it is being estimated from interparticle porosity (ε_{bed}).

The last resistance will be intraparticle MT resistance. At this level, the consideration of Knudsen diffusion is crucial. The reason is if the pore diameter (d_{pore}) is smaller than the mean free path (λ), instead of conventional diffusion (D_{CO2}) Knudsen diffusion (D_K) will occur. Therefore, to determine the dominating mode of diffusion, the model has the functionality where it calculates the Knudsen number (K_n) and based on that determines the mode of diffusion. If K_n is less than 0.1, Knudsen diffusion will occur. If K_n is greater than 10 then conventional diffusion will take place. In between those regions, simply an average of both diffusions will be calculated and considered [49].

$$K_n = \frac{d_{pore}}{\lambda} \quad (12)$$

$$\lambda = \frac{3.2\,\mu}{P}\left(\frac{RT}{2\pi M}\right)^{1/2} \quad (13)$$

$$D_{particle} = \frac{\varepsilon_{particle} D_{CO2}}{\tau_{particle}} \quad (If\ K_n > 10) \quad (14)$$

$$D_K = 48.5 d_{pore}\left(\frac{T}{M}\right)^{1/2} \quad (15)$$

$$D_{particle} = \frac{\varepsilon_{bed} D_K}{\tau_{particle}} \quad (If\ K_n < 0.1) \quad (16)$$

$$D_{particle} = \frac{1}{\frac{1}{D_{CO2}} + \frac{1}{D_K}} \quad (If\ 0.1 \leq K_n \leq 10) \quad (17)$$

The overall mass transfer coefficient (k) will be calculated with eq. 18 after identifying individual mass transfer coefficients.

$$\frac{1}{k} = \frac{1}{k_{interphase}} + \frac{S/2}{D_{bed}} + \frac{d_{particle}/2}{D_{particle}} \quad (18)$$

Mass Balance:

In this step, the overall balance for CO_2 will take place to determine the loading rate of CO_2 in the sorbent. It will also help us determine the outlet CO_2 concentration from each of the finite elements that will become the input for the next one. Since the model is applicable in the turbulent region, the simplified mass balance can be written as given in eq. 19.

$$F_{air}\left[C_{CO2(in)} - C_{CO2(out)}\right] = A\rho_{bed}k(Q_{CO2}^{eq} - Q_{CO2}) \quad (19)$$

$$Q_{CO2} = \frac{q_{sat1T_{regen}} b_{1T_{regen}} p_{CO2(regen)}}{1 + b_{1T_{regen}} p_{CO2(regen)}} + b_{2T_{regen}} p_{CO2(regen)} \quad (20)$$

$$Q_{CO2}^{eq} = \frac{q_{sat1} b_1 p_{CO2}}{1 + b_1 p_{CO2}} + b_2 p_{CO2} \quad (21)$$

The equilibrium CO_2 loading (Q_{CO2}^{eq}) will depend on the ambient process conditions as given in eq. 21. The model currently uses modified Toth isotherm [19] as the sorbent selected for current modelling (MIL-101(Cr)) follows that. This isotherm can be converted to Langmuir isotherm by setting up $b_2 = 0$ in Eq. 21. On the other hand, the initial loading of CO_2 in the sorbent (Q_{CO2}) will be determined by set regeneration

conditions given in the inputs and using eq. 20. This will make the future addition of regeneration modelling into the current model easier. This step will create a package of calculations that will be used repetitively for each finite element defined in the model for the channel in step 5.

Formulating Results:

Iterative calculations will be performed in this step to generate results for CO_2 loading rate, Outlet CO_2 concentration, and CO_2 loading in the sorbent. The package of calculations constructed in Step 4 will be utilized here. In equilibrium mode, the model will run the code until the last element approaches equilibrium as per the set target. Similarly, in the defined cycle time mode it will run for a set number of seconds.

In this step, the model generates a considerable amount of data from calculations. To handle this effectively, it creates a master list for each time instance followed by a sub-list for each finite element where it will store values for all the above-mentioned parameters for each time instance. These lists then will be converted to arrays in Python to obtain structured results.

Data Visualization:

For any study, the obtained results are more digestible if they are visualized in the form of graphs. Data visualization helps with analyzing the performance of the asset by understanding what is going on in the system. In this step, data from arrays generated in

step 5 will be used to create graphs. Major graphs generated from the model are for unit cell loading, cumulative/total channel loading, average driving force, and breakthrough curve. All these graphs generated for the input given in Table 2 are shown and explained below.

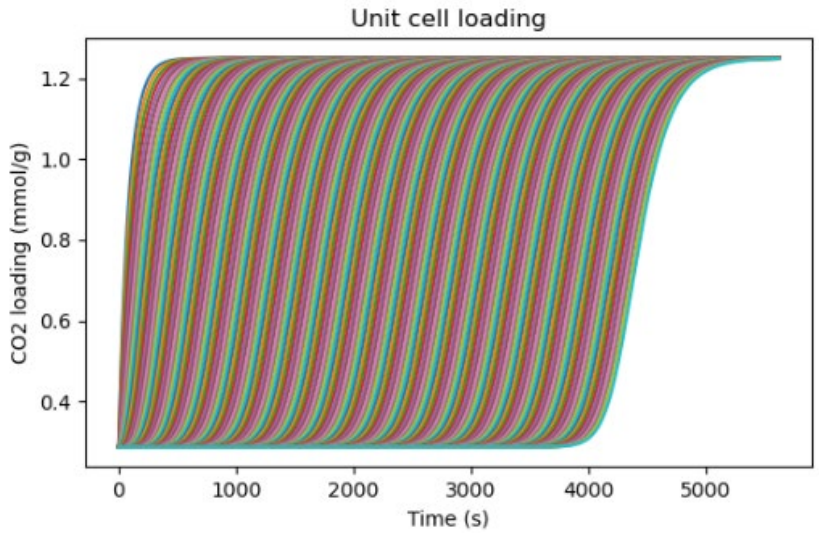

Figure 7. Unit Cell loading curves

The unit cells loading curve for a 0.2 m long bed is given in Figure 7. This graph helps in understanding the loading of each finite element in the contactor channel. It also gives information about the effective operating range for the sorbent material. It can help understand the profile of CO_2 loading for the contactor channel over time.

The channel loading curve is generated by adding instantaneous finite element loading in the channel for each timeframe. This will give information about the effective capacity of the contactor channel to capture CO_2 from the air. The channel loading curves at different ambient conditions can be used to understand the sensitivity of the channel's capture

capacity in various ambient conditions that can help determine capacity fluctuations. This in turn can help optimize the geometry of the channel.

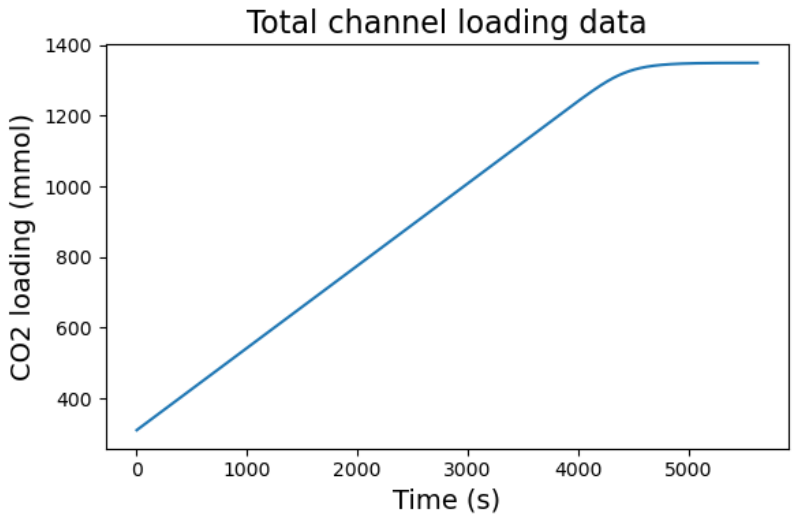

Figure 8. Total channel loading curve

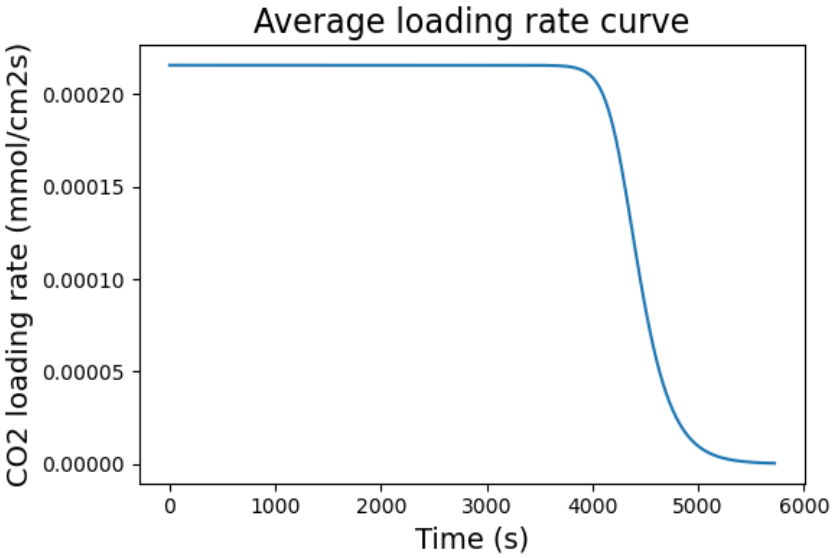

Figure 9. Average loading rate curve

The average driving force curve is generated by taking an average of finite element driving force data. This is shown in Figure 9. This graph is very important in determining the best operating range and corresponding cycle time for the capture step of the air contactor. In the design stage, this can help the user adjust the length and thickness of the channel to get the best performance in the prevailing ambient conditions.

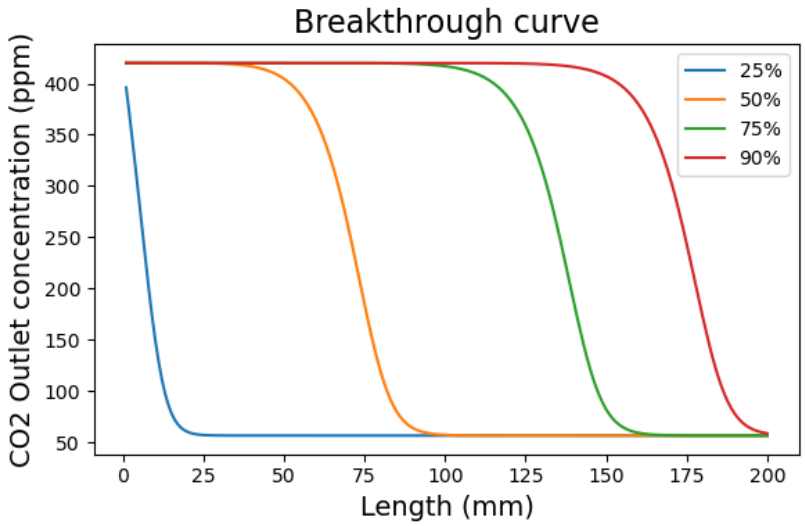

Figure 10. Breakthrough curve at different loading levels (25%, 50%, 75% and 90% of net loading)

Breakthrough curves are shown in Figure 10. Current visualization gives information about channel CO_2 concentration at 25%, 50%, 75%, and 90% of net loading capacity. Breakthrough curves give valuable information about the effective mass transfer zone in the channel at given instances. This also helps optimize the geometry of the channel based on prevailing ambient conditions for maximum CO_2 extraction.

Final Report Creation:

This is the last step in the modelling process where all the important information from the modelling is showcased in the form of a report. The model generates the report in .pdf format. The sample design result report for input conditions given in Table 2 is shown in Appendix B.

As shown, this will consist of inputs for ambient conditions, a channel diagram with dimensions, calculated mass transfer results, a total channel loading curve, an average driving force curve, and a breakthrough curve with a table of average process parameters. This report will help users understand the performance of the contactor easily and make design changes as required to optimize the design of the channel for efficient CO_2 capture.

CHAPTER 5

ROBUSTNESS CHECK AND SENSITIVITY ANALYSIS

The previous section explained the model development for the capture step of the DAC contactor. It is important to validate that the model is working appropriately in the applicable operating range. To ensure this, a robustness check is performed. During this analysis, any discrepancies observed were analyzed and interpreted accordingly to address the concern. Table 3 gives a highlight of this activity. It is good to report that the model performance was satisfactory in the applicable range of operation, without any breakdowns. Resolution adjustment is required in several instances to eliminate fluctuations and to prevent reversal of driving forces.

Table 3. Robustness check highlights table

Sr No.	**Parameter**	**Comment on model performance**
1	Ambient Temperature *(T)*	Resolution adjustment is required if the model shows fluctuations
2	Ambient Pressure *(P)*	Model performs satisfactorily
3	Air Velocity *(v)*	Velocity should be such that the model remains in the turbulent region.
4	Length of channel *(L)*	The model response gets sluggish when the number of finite elements goes above 1000.
5	Width of channel *(W)*	The model performs satisfactorily.
6	Thickness of the bed *(S)*	The model performs satisfactorily.
7	Height of channel *(H)*	Height should be such that the model remains in the turbulent region.
8	Particle pore diameter *(d_{pore})*	The model performs satisfactorily.
9	Regeneration Temperature *(T_{regen})*	T_{regen} should be sufficiently high to maintain a positive driving force.

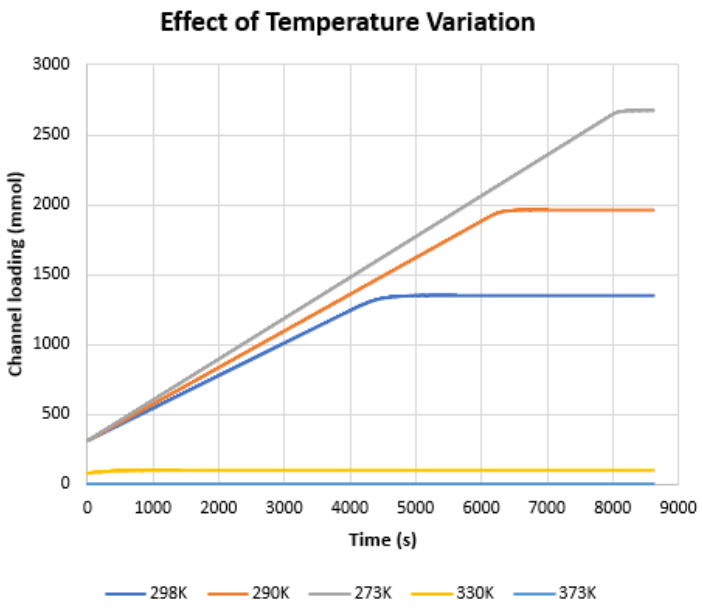

Figure 11. Effect of ambient temperature on channel loading

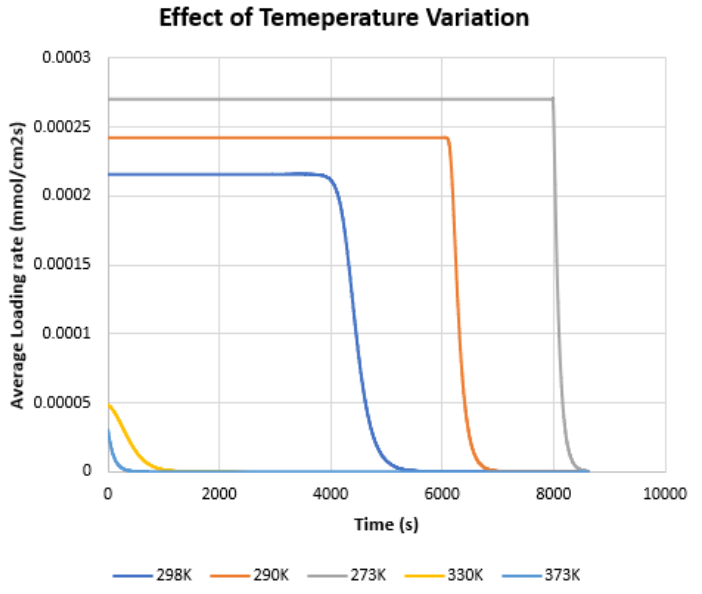

Figure 12. Effect of ambient temperature on loading rate, for 273K, 290K, 298K, 330K and 373K

The robustness check is also performed for the width of the channel, pore particle diameter, and CO_2 ppm level. The model performed satisfactorily for those variations as well.

The sensitivity analysis is carried out to understand the impact process parameters on the contactor performance for DAC. For this, each input is varied independently to some extent, and a change in performance is observed. The base case will remain the same as explained in table 2.

Effect of Ambient Temperature Change:

The change in ambient temperature has a drastic effect on the performance of the DAC contactor. From Figure 11 and 12, it is evident that the channel capacity increases with decreasing temperature and the same is true for driving force. The reason is the effect of temperature on the equilibrium loading. From Table 4, the final equilibrium loading increases with decreasing temperature which leads to increased capacity and higher average driving force. Another point to clarify from a modelling perspective is that as the temperature goes down, the resolution needs to be adjusted to predict the correct performance. This is where there are chances that the model may start taking more time to run the model due to the increased number of finite elements. The model is tested at 330 K which is the highest recorded temperature on the earth. The model was also tested at one of the regeneration conditions for capture at 373K to ensure its sturdiness and it is good to report that it worked appropriately in all these conditions.

Table 4. Effect of temperature on equilibrium loading

Temperature (K)	Initial loading (mmol/g)	Final loading (mmol/g)
273	0.2873	2.4743
290	0.2873	1.8161
298 *(base case)*	0.2873	1.2496
330	0.0731	0.0925
373	0	0.0031

Effect of Ambient Pressure Change:

The sensitivity of ambient pressure was tested by considering different values based on geographical elevation. This is shown in Figures 13 and 14 for five different conditions. The average pressure for Phoenix, Flagstaff, La Rinconada (highest human habitant), and Mt. Everest are taken by considering corresponding elevations. Then, a low-pressure condition of 100 Pa was also tested to ensure that the model works satisfactorily in vacuum conditions as well. The model ran without any concerns. From the graphs, as pressure decreases the channel loading and loading rate both decrease due to a reduction in equilibrium loading. Table 5 gives more clarity on this. From the results, the elevation has a considerable effect on the performance of DAC contactors. It is also known that two of the locations: La Rinconada and Mt. Everest are not physically viable places to set up the DAC facility, but the purpose here is to show that theoretically, if these conditions are chosen then also the model runs satisfactorily.

Table 5. Effect of pressure on equilibrium loading

Pressure (Pa)	Initial loading (mmol/g)	Final loading (mmol/g)
98000 (Phoenix) *(base case)*	0.2873	1.2496
79800 (Flagstaff)	0.2873	1.1172
56404 (La Rinconada)	0.2873	0.9033
34900 (Mt. Everest)	0.2873	0.6443
100 (Vacuum condition)	0	0.0026

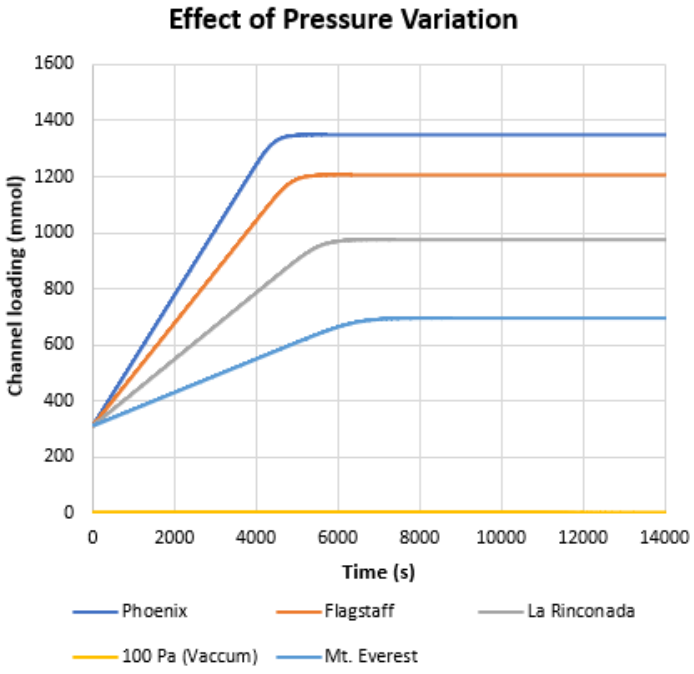

Figure 13. The effect of Pressure on Total Channel Loading at 298K

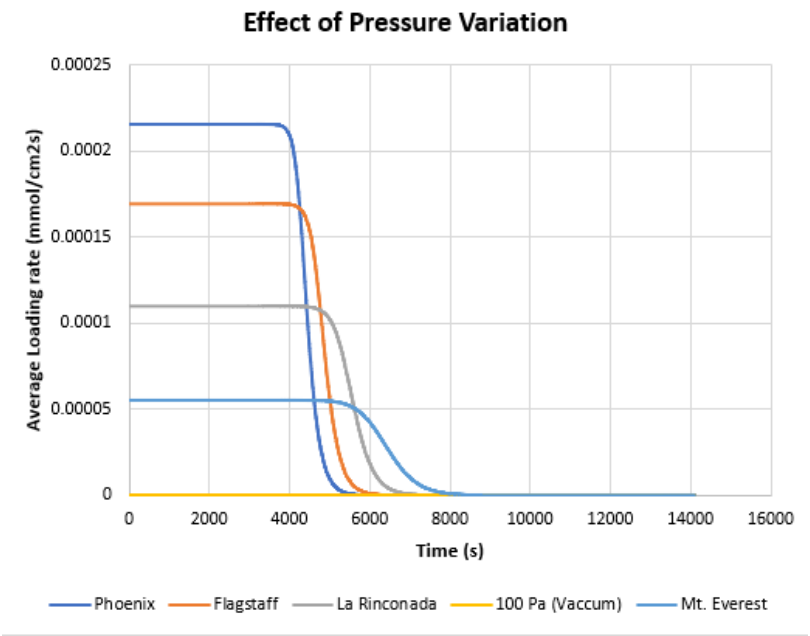

Figure 14. Effect of pressure on the loading rate at 298K

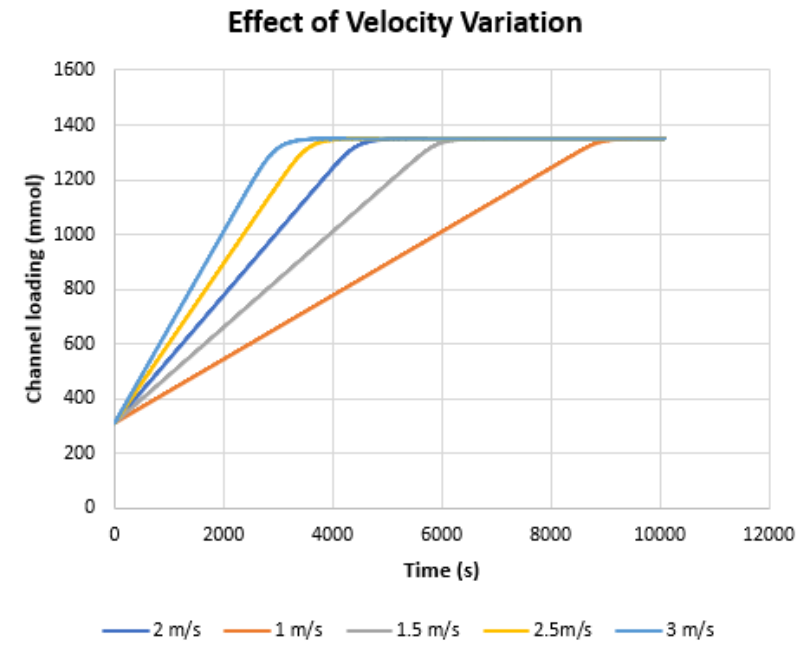

Figure 15 Effect of velocity on channel loading at 98000Pa and 298K

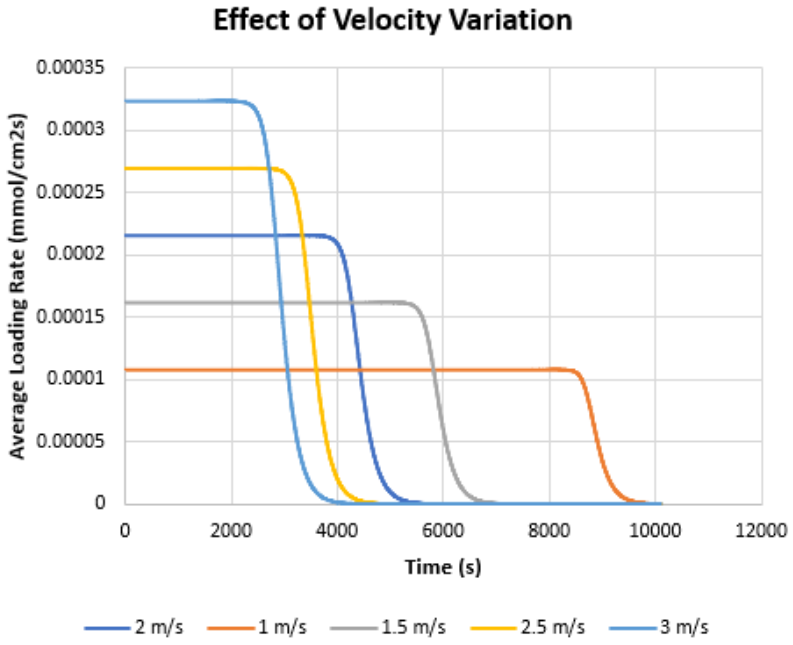

Figure 16 Effect of velocity on average driving force at 98000 Pa and 298K

Effect of Channel Velocity Change:

Figures 15 and 16 explain the effect of channel velocity on the loading level and CO_2 loading rate. It is expected that as velocity increases capacity to remain intact because it does not affect the equilibrium. Conversely, the time for loading decreases due to a rise in mass flow rate in the channel. Table 6 highlights the effect on N_{Re} and interphase MT coefficient from this change. Therefore, the model performance meets expectations. A point of caution is that the current model is applicable to the turbulent region, so the model will require to alert the user if the condition becomes laminar in the channel. Even though 1 m/s velocity creates laminar conditions here it is being considered. The reason is to showcase the model's robustness and future applicability in the laminar region if the gas phase gradient is taken into consideration.

Table 6. The effect of velocity on Reynold's number and interphase MT coefficient

Velcocity (m/s)	**Reynold's number**	**Interphase MT coefficient (m/s)**
2 *(base case)*	7484	0.0201
1	3742	0.0113
1.5	5613	0.0159
2.5	9356	0.0243
3	11227	0.0282

Effect of Channel Thickness Change:

Channel thickness affects the total channel capacity and in turn the loading time and rate. Graphs in Figures 17 and 18 illustrate these changes and their effects on the performance of the contactor channel. As thickness decreases the channel capacity decreases (Figure 17) due to less amount of sorbent material present per unit area for mass transfer. Also, it has a considerable effect on the average loading rate as per Figure 18. The curve becomes more upright which indicates that near the breakthrough point, as thickness decreases almost the whole channel becomes saturated which indicates higher bed utilization. A clarification is required here for the model resolution. The resolution is adjusted for decreased thickness to prevent unwanted oscillations which is a result of frequent reversal of driving force that is practically not feasible in the real-world capture stage in DAC. Due to higher resolution, it is observed that the model response becomes sluggish as the model has a greater number of finite elements to deal with.

Table 7 gives more details about how the change in thickness can impact the overall production rate of the DAC contactor. The comparison indicates that thinner channels can lead to improved productivity for the same amount of sorbent material.

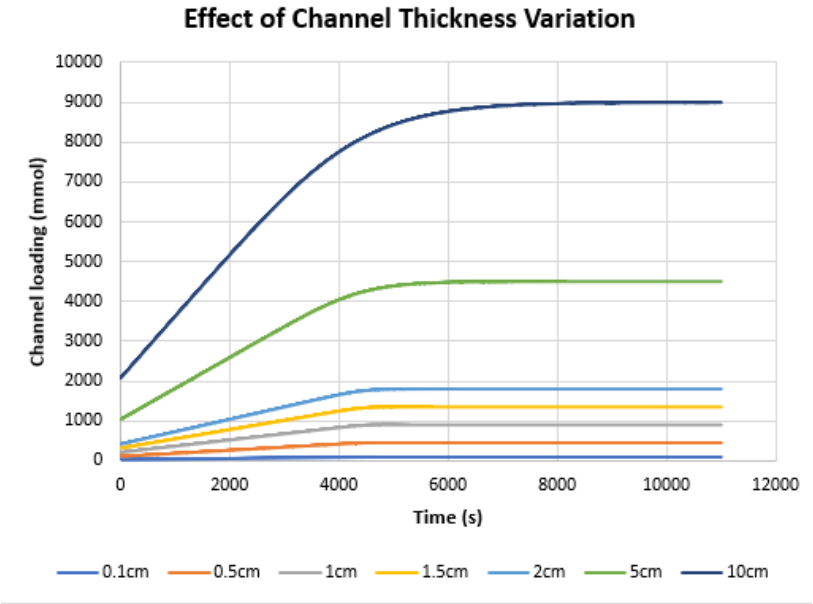

Figure 17. Effect of channel thickness at 98000 Pa and 298 K

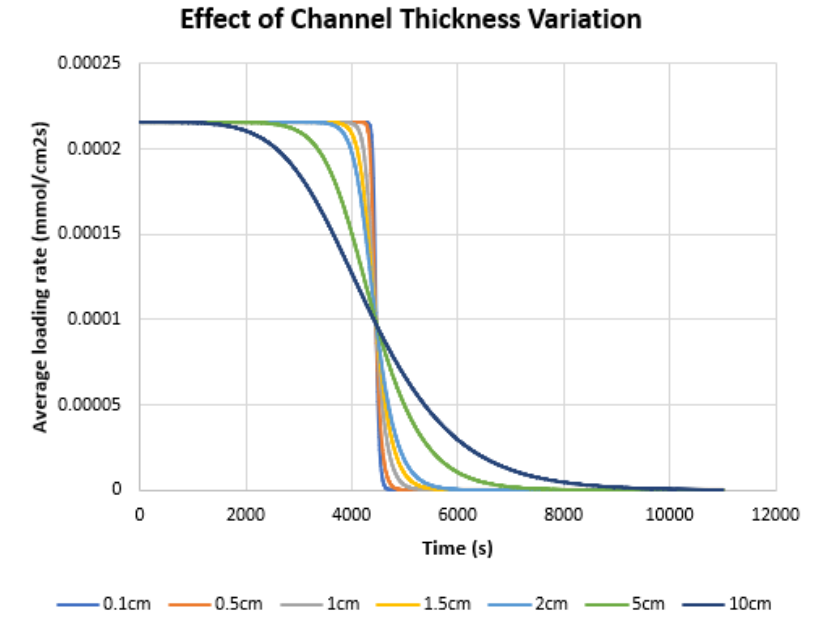

Figure 18 Effect of Channel thickness on the average loading rate at 98000 Pa and 298 K

Table 7. Effect of channel thickness of the contactor on the daily capture capacity

Thickness (cm)	Sorbent mass per channel (kg)	No. of channels	Total mass of sorbent (kg)	Cycle time	Daily possible cycles	Daily capacity (mol/kg)
10	7.200	1	7.2	11003	6	5.7738
5	3.600	2	7.2	8143	8	7.6984
2	1.440	5	7.2	6107	10	9.623
1.5	1.080	7	7.56	5724	11	10.5853
1	0.720	10	7.2	5328	12	11.5476
0.5	0.360	20	7.2	4925	12	11.5476
0.1	0.072	100	7.2	4707	13	12.5099

This shows the way of design optimization for efficient DAC contactor design. The point of consideration will be the structural strength of the contactor that needs to be addressed separately.

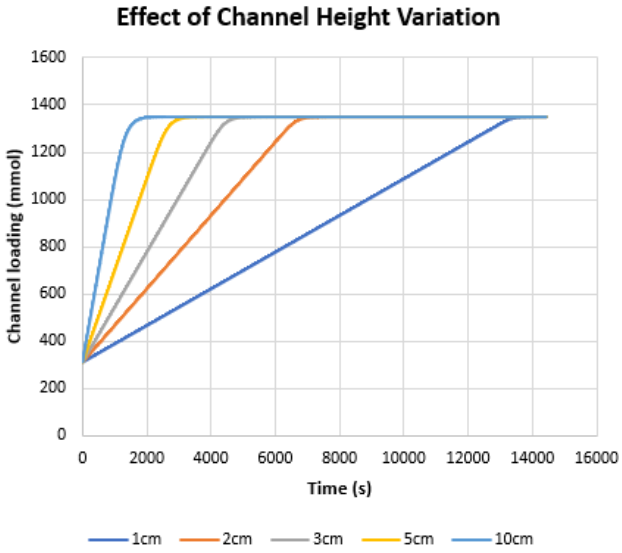

Figure 19. Effect of Channel Height on Loading Rate at 98000 Pa and 298 K

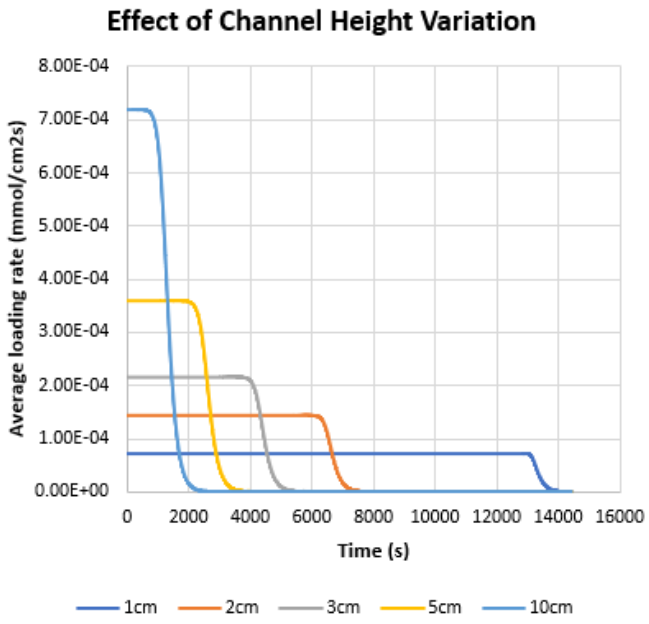

Figure 20. Effect of channel height on driving force at 98000 Pa and 298 K

Effect of channel height change:

The impact of channel height change is like the velocity change as shown in Figures 19 and 20. As the height increases, the volume of air passing through the channel increases, and that increases the loading rate of CO_2 in the channel. This is also one of the optimization knobs for the contactor design where the contactor size will be a controlling factor.

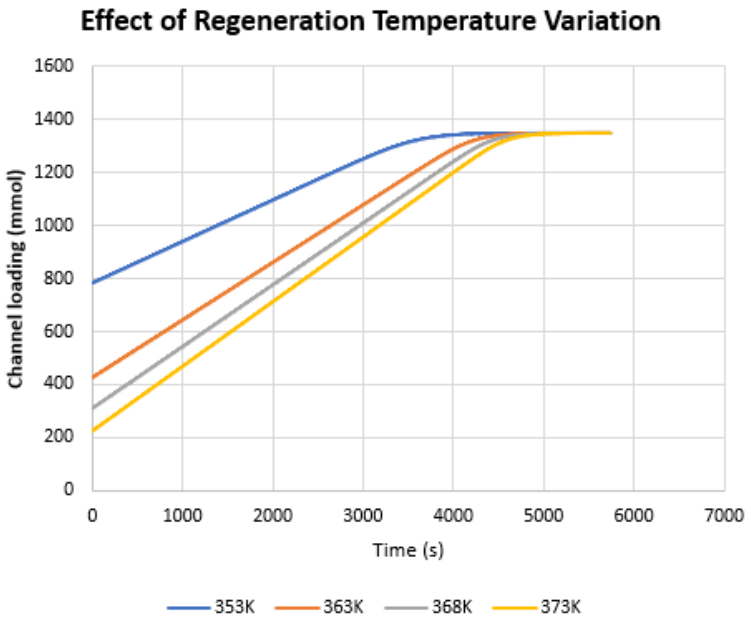

Figure 21. Effect of regeneration temperature at 98000 Pa and 298 K

Effect of Regeneration Temperature:

Defining regeneration conditions makes the model performance more realistic as that will provide the real-world operating range in which the system is going to operate. Regeneration conditions affect the initial loading of the sorbent material. Table 7 gives a better idea about the effect on the initial loading of the sorbent material. A sensitivity analysis for this is also performed to analyze the impact. From the analysis, it can be said that the model performed satisfactorily for any feasible T_{regen} which maintains a positive driving force in the model. Graphs in Figure 21 and 22 show more operating range for the sorbent with higher T_{regen} and improved performance of the DAC contactor.

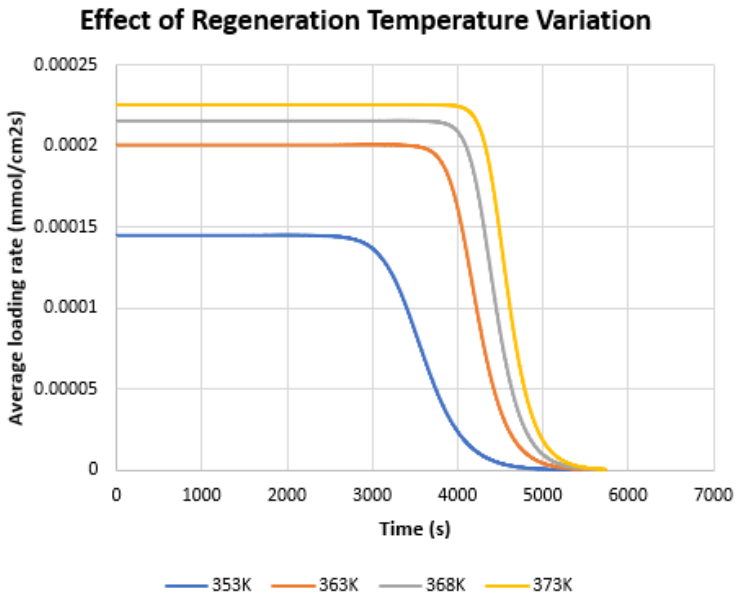

Figure 22. The change in the average driving force for CO2 with regeneration temperature at 98000 Pa and 298 K

Table 8. Effect of regeneration temperature on initial loading of the sorbent material

Regeneration Temperature (T_{regen}) (K)	**Initial loading (mmol/g)**
353	0.7249
363	0.3952
368 (*base case*)	0.2873
373	0.2082

Until now all the analysis has been conducted with changing one process input. But in real world operations, more than one of these could change. These types of analyses can give a more comprehensive idea of the DAC contactor performance in the real world. The weather data for three locations: Phoenix, Tucson, and Flagstaff was tested with the model to understand the effect of changing ambient conditions. Graphs in Figure 23 give highlights of this comparison. Historical average weather data (temperature, pressure, and

wind speed) for the start of first four weeks of the October is taken from the internet [51]. The same geometry identified in the base case is used here. The regeneration temperature is 373K. The purpose here is to showcase one of the applications for the model.

Table 9. Performance estimation from the model based on obtained cycle time and loading capacity.

PHOENIX						
	Cycle time (s) T max	**Possible No. of Cycles per day**	**Daily CO2 capture (mol/kg)**	**Cycle time (s) T min**	**Possible No. of Cycles per day**	**Daily CO2 capture (mol/kg)**
Week 1	5100	16	6.47	6511	13	16.24
Week 2	5273	16	8.12	6618	13	18.07
Week 3	5614	15	10.29	6946	12	19.14
Week 4	5820	14	11.44	7154	12	20.64
TUSCON						
	Cycle time (s) T max	**Possible No. of Cycles per day**	**Daily CO2 capture (mol/kg)**	**Cycle time (s) T min**	**Possible No. of Cycles per day**	**Daily CO2 capture (mol/kg)**
Week 1	5176	16	7.77	6609	13	18.62
Week 2	5336	16	9.58	6699	12	18.82
Week 3	5473	15	10.84	6862	12	21.06
Week 4	5586	15	12.85	6822	12	21.73
FLAGSTAFF						
	Cycle time (s) T max	**Possible No. of Cycles per day**	**Daily CO2 capture (mol/kg)**	**Cycle time (s) T min**	**Possible No. of Cycles per day**	**Daily CO2 capture (mol/kg)**
Week 1	7096	12	15.05	8976	9	19.17
Week 2	7537	11	15.39	9078	9	19.67
Week 3	7674	11	16.92	9155	9	20.07
Week 4	7955	10	16.68	9185	9	20.24

This analysis helped in calculating the possible number of cycles that can be performed each day. If the regeneration cycle time is fixed i.e., 30 minutes with an assumption of

100% removal of captured CO_2 then table 8 gives a highlight of performance prediction of the designed channel. Here, the results will be more useful if an optimized cycle is used based on operations decision. The purpose here is to showcase the usefulness and user friendliness of the model. The advantages and more usefulness will be explained later.

From the robustness check, it is concluded that the model runs satisfactorily and as per expectation for all input parameters. Alerts and notifications are implemented in the model to notify the user whenever conditions change. Another point of consideration is the selection of appropriate model resolution. This is required to prevent unwanted oscillations in the CO_2 loading and reversal of driving in the capture step which is practically not feasible.

From the sensitivity analysis, it was found that ambient conditions and geographical location has considerable effect on the DAC contactor performance. To get the most of changing ambient conditions, the geometry of channel, i.e., wall thickness, channel height, length and channel properties are crucial parameters that can be optimized. All these studies of sensitivity of DAC have been performed discretely in literature before. The purpose here is to showcase the capability to perform all these analyses in a user-friendly manner. The model gives maximum flexibility to the user and ease of changing process parameters to analyze the performance of their designs. It will help in understanding factors that need to be optimized to design an efficient contactor.

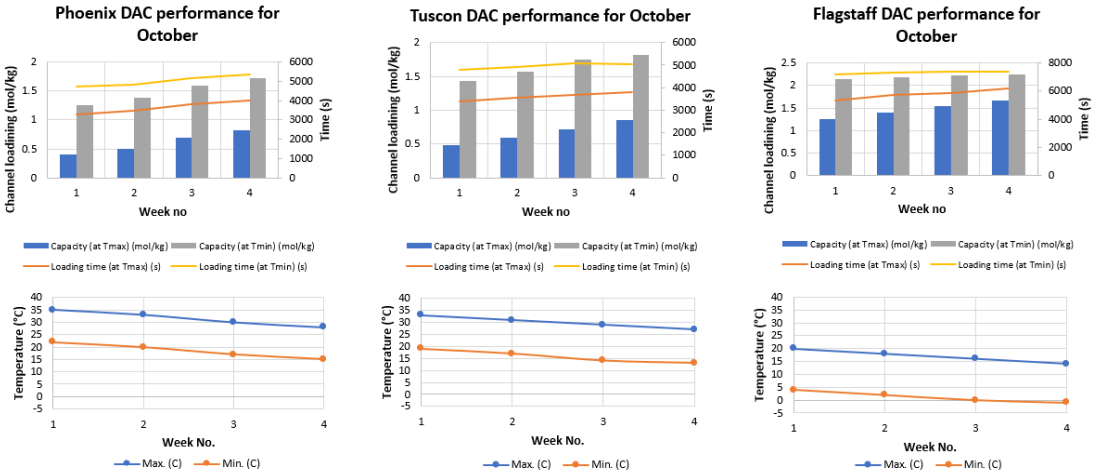

Figure 23. The performance of the DAC contactor channel at different locations

CHAPTER 5

CONCLUSION

The data of current energy trends clearly showed that more than two-thirds of the world's energy demand is being fulfilled by fossil fuels which is causing a rise in CO_2 emissions reaching ~35 Gt/yr. This showed us the importance and the need for CCUS and CDR technologies to reduce and clean up emissions caused by human activities. Direct Air Capture is one of the CDR approaches that has tremendous potential but is currently facing issues that any early-stage chemical technology normally faces. Current concerns are around the need for cheap and efficient material, higher cost for CO_2 capture, and assurance of net negative emissions throughout the life cycle. Process Modelling is a proven approach that will help resolve these by catalyzing the research pace and can help save a considerable amount of time and money.

This work has tried to provide a unique direction in terms of developing a model from the user standpoint to give researchers, designers, and engineers maximum flexibility to design DAC contactors. The formulated model has versatility for defining process conditions, independence of defining or selecting geometry for the DAC contactor, and the option to take in any known sorbent material.

The model is created in Python and the flow of information in the model is explained by elaborating each step. The equation and empirical correlation used to make it flexible enough to model any known geometry are then explained. A robustness check is then

performed to ensure that the model works without any breakdown. Results clearly indicated that the modelling was successful without any breakdowns. Concerns on oscillations and negative CO_2 concentration in the air are addressed with resolution increment.

Sensitivity analysis showed potential advantages the model can provide are as follows.

- Rapid sorbent screening for the selected geometry and for the opted geographic locations to select the best sorbent or sorbent combinations. E.g., the Department of Energy's DAC Hub, CarbonCapture's Project Bison or any other DAC project planned to set up near sequestration sites could use this for making design decisions.
- For sorbent vendors, it can help tailor their existing sorbent portfolio by modifying or adding new materials, based on identified geographical sites. From the geometry perspective, it can help them design or alter chemistry that can give the best performance for the given form factor.
- At the research stage, the model can help with identifying new designs for the contactor and virtually validating the design before actually making one which can save a considerable amount of time and money by reducing redundancy and revisions. This can also reduce failures and help design effective DAC contactors with lower pressure drop, high capture efficiency, and net negative footprint.
- Developed modular designs with the model can be easily scaled up for large-scale deployment of DAC.

- For a properly defined system, it can help forecast the performance of the asset as DAC is highly weather dependent (Figure 23). This will be useful in optimizing the cycle times of clusters.

The final aim will be to provide a digital platform that can help create, test, and simulate cost-effective, scalable, and deployable DAC contactor designs to clean up anthropogenic emissions and mitigate global warming.

CHAPTER 7

FUTURE DIRECTIONS

As per Frontier's CDR gaps [52], research is needed to design cheap and efficient DAC contactors for large-scale deployment. This modelling approach is a long-term effort to create a user-friendly generalized process modelling package for solid sorbent DAC contactors. The current work was to develop a generalized mass transfer model for the capture step in the DAC process. The current model needs to be improvised by inclusion of bulk phase resistance to include laminar region modelling. The addition of pressure drop calculation can be of real value. In continuation, various regeneration schemes will be generated to integrate it with the current model to complete the package for DAC contactor design, modelling, and simulation. Also, it is required to ensure that the model performance imitates the actual system. Therefore, work will be done to validate the performance of the model with the real-world system. There are so many avenues that can be explored with the process model as per the DAC-DT concept which can help set up a base foundation for the digital eco-system for DAC. Approaches that currently look more promising are: The creation of a sorbent library to help test different sorbents or sorbent combinations and select the best options that can be deployed in the given conditions, develop a location-based weather historian that can facilitate past or current weather data which can be fed to the model to predict the DAC contactor performance.

REFERENCES

1. IPCC, 2014: Summary for Policymakers. In: Climate Change 2014: Mitigation of Climate Change. Contribution of Working Group III to the Fifth Assessment Report of the Intergovernmental Panel on Climate Change [Edenhofer, O., R. Pichs-Madruga, Y. Sokona, E. Farahani, S. Kadner, K. Seyboth, A. Adler, I. Baum, S. Brunner, P. Eickemeier, B. Kriemann, J. Savolainen, S. Schlömer, C. von Stechow, T. Zwickel and J.C. Minx (eds.)]. Cambridge University Press, Cambridge, United Kingdom and New York, NY, USA

2. IPCC, 2023: Summary for Policymakers. In: Climate Change 2023: Synthesis Report.Contribution of Working Groups I, II, and III to the Sixth Assessment Report of the Intergovernmental Panel on Climate Change [Core Writing Team, H. Lee and J. Romero (eds.)]. IPCC, Geneva, Switzerland, pp. 1-34, doi: 10.59327/IPCC/AR6-9789291691647.001

3. Energy Institute, 2023 Statistical Review of Energy, September 25, 2023, https://www.energyinst.org/statistical-review

4. Canadell, J.G., P.M.S. Monteiro, M.H. Costa, L. Cotrim da Cunha, P.M. Cox, A.V. Eliseev, S. Henson, M. Ishii, S. Jaccard, C. Koven, A. Lohila, P.K. Patra, S. Piao, J. Rogelj, S. Syampungani, S. Zaehle, and K. Zickfeld, 2021: Global Carbon and other Biogeochemical Cycles and Feedbacks. In Climate Change 2021: The Physical Science Basis. Contribution of Working Group I to the Sixth Assessment Report of the Intergovernmental Panel on Climate Change [Masson-Delmotte, V., P. Zhai, A. Pirani, S.L. Connors, C. Péan, S. Berger, N. Caud, Y. Chen, L. Goldfarb, M.I. Gomis, M. Huang, K. Leitzell, E. Lonnoy, J.B.R. Matthews, T.K. Maycock, T. Waterfield, O. Yelekçi, R. Yu, and B. Zhou (eds.)]. Cambridge University Press, Cambridge, United Kingdom and New York, NY, USA, pp. 673–816, doi: 10.1017/9781009157896.007.

5. Steve Rackley, Chapter 11 - Afforestation and other land- and soil-based methods, Editor(s): Steve Rackley, Graham Andrews, Diarmaid Clery, Renaud De Richter, George Dowson, Pol Knops, Wei Li, Stephen Mccord, Tingzhen Ming, Adrienne Sewel, Peter Styring, Michael Tyka, Negative Emissions Technologies for Climate Change Mitigation, Elsevier, 2023, Pages 215-248, ISBN 9780128196632, https://doi.org/10.1016/B978-0-12-819663-2.00018-6.

6. Lal, R. (2020). Managing soils for negative feedback to climate change and positive impact on food and nutritional security. Soil Science and Plant Nutrition, 66(1), 1–9. https://doi.org/10.1080/00380768.2020.1718548

7. Kwang Ho Kim, Tae-Seung Kim, Soo-Min Lee, Donha Choi, Hwanmyeong Yeo, In-Gyu Choi, Joon Weon Choi, Comparison of physicochemical features of biooils and biochars produced from various woody biomasses by fast pyrolysis, Renewable Energy, Volume 50, 2013, Pages 188-195, ISSN 960-1481, https://doi.org/10.1016/j.renene.2012.06.030

8. Johannes Lehmann, Matthias C. Rillig, Janice Thies, Caroline A. Masiello, William C. Hockaday, David Crowley, Biochar effects on soil biota – A review, Soil Biology and Biochemistry, Volume 43, Issue 9, 2011, Pages 1812-1836, ISSN 0038-0717, https://doi.org/10.1016/j.soilbio.2011.04.022

9. Freeman, C., Fenner, N., & Shirsat, A. H. (2012). Peatland geoengineering: An alternative approach to terrestrial carbon sequestration. Philosophical Transactions of the Royal Society A: Mathematical, Physical and Engineering Sciences, 370(1974), 4404–4421. https://doi.org/10.1098/rsta.2012.0105

10. Mcleod, E., Chmura, G.L., Bouillon, S., Salm, R., Björk, M., Duarte, C.M., Lovelock, C.E., Schlesinger, W.H. and Silliman, B.R. (2011), A blueprint for blue carbon: toward an improved understanding of the role of vegetated coastal habitats in sequestering CO_2. Frontiers in Ecology and the Environment, 9: 552-560. https://doi.org/10.1890/110004

11. Jürchott, M., Oschlies, A., & Koeve, W. (2023). Artificial upwelling—A refined narrative. Geophysical Research Letters, 50, e2022GL101870. https://doi.org/10.1029/2022GL101870

12. Smetacek V and Naqvi S.W.A 2008The next generation of iron fertilization experiments in the Southern OceanPhil. Trans. R. Soc. A.3663947–3967 http://doi.org/10.1098/rsta.2008.0144

13. Haroon S. Kheshgi, Sequestering atmospheric carbon dioxide by increasing ocean alkalinity, Energy, Volume 20, Issue 9, 1995, Pages 915-922, ISSN 0360-5442, https://doi.org/10.1016/0360-5442(95)00035-F

14. Schuiling, R. D., & Krijgsman, P. (2006). Enhanced weathering: An effective and cheap tool to sequester CO2. *Climatic Change*, *74*(1–3), 349–354. https://doi.org/10.1007/s10584-005-3485-y

15. Friedmann, S. J., A. Zapantis, B. Page, C. Consoli, Z. Fan, I. Havercroft, H. Liu, E. Ochu, N. Raji, and D. Rassool. "Net-Zero and Geospheric Return: Actions Today for 2030 and Beyond; SIPA Center on Global Energy Policy: New York,

NY, USA, 2020. https://www.globalccsinstitute.com/wp-content/uploads/2020/09/Netzero-and-Geospheric-Return-2.pdf

16. Rui-Long Wang, Ming-Jia Li, Dong Li, Yi-Wen Yang, The synergy of light/fluid flow and membrane modification of a novel membrane microalgal photobioreactor for direct air carbon capture, Applied Energy, Volume 328, 2022, 120133, ISSN 0306-2619, https://doi.org/10.1016/j.apenergy.2022.120133

17. Mohammad Ali Zahed, Elaheh Movahed, Arezoo Khodayari, Saba Zanganeh, Maryam Badamaki, Biotechnology for carbon capture and fixation: Critical review and future directions, Journal of Environmental Management, Volume 293, 2021, 112830, ISSN 0301-4797, https://doi.org/10.1016/j.jenvman.2021.112830

18. Ahmed Sodiq, Yasser Abdullatif, Brahim Aissa, Arash Ostovar, Nashaat Nassar, Muftah El-Naas, Abdulkarem Amhamed, A review on progress made in direct air capture of CO2, Environmental Technology & Innovation, Volume 29, 2023, 102991, ISSN 2352-1864, https://doi.org/10.1016/j.eti.2022.102991

19. Sinha, A., Darunte, L. A., Jones, C. W., Realff, M. J., & Kawajiri, Y. (2017). Systems design and economic analysis of Direct Air Capture of CO2 through temperature vacuum swing adsorption using MIL-101(CR)-PEI-800 and mmen-mg2(dobpdc) MOF adsorbents. Industrial & Engineering Chemistry Research, 56(3), 750–764. https://doi.org/10.1021/acs.iecr.6b03887

20. Jan Andre Wurzbacher, Christoph Gebald, Samuel Brunner, Aldo Steinfeld, Heat and mass transfer of temperature–vacuum swing desorption for CO2 capture from air, Chemical Engineering Journal, Volume 283, 2016, Pages 1329-1338, ISSN 1385-8947, https://doi.org/10.1016/j.cej.2015.08.035

21. Xuancan Zhu, Tianshu Ge, Fan Yang, Ruzhu Wang, Design of steam-assisted temperature vacuum-swing adsorption processes for efficient CO2 capture from ambient air, Renewable and Sustainable Energy Reviews, Volume 137, 2021, 110651, ISSN 1364-0321, https://doi.org/10.1016/j.rser.2020.110651

22. Z.X. Zhang, H.J. Xu, W.S. Hua, C.Y. Zhao, Thermodynamics analysis of multi-stage temperature swing adsorption cycle for dilute CO2 capture, enrichment and purification, Energy Conversion and Management, Volume 265, 2022, 115794, ISSN 0196-8904, https://doi.org/10.1016/j.enconman.2022.115794

23. Lackner, Klaus, and Peter Schulze. "Autothermal direct air capture system." U.S. Patent Application 17/912,486 filed May 25, 2023.

24. Tao Wang, Xinru Wang, Hao Dong, Kun Ge, Klaus Lackner, Moisture swing frequency response method for characterization of ion-transport kinetics of CO2 adsorption, International Journal of Heat and Mass Transfer, Volume 216, 2023, 124551, ISSN 0017-9310, https://doi.org/10.1016/j.ijheatmasstransfer.2023.124551

25. Qingdian Shu, Ching Shing Sin, Michele Tedesco, Hubertus V.M. Hamelers, Philipp Kuntke, Optimization of an electrochemical direct air capture process with decreased CO2 desorption pressure and addition of background electrolyte, Chemical Engineering Journal, Volume 470, 2023, 144251, ISSN 1385-8947, https://doi.org/10.1016/j.cej.2023.144251

26. Carsten Drechsler, David W. Agar, Simulation and optimization of a novel moving belt adsorber concept for the direct air capture of carbon dioxide, Computers & Chemical Engineering, Volume 126, 2019, Pages 520-534, ISSN 0098-1354, https://doi.org/10.1016/j.compchemeng.2019.04.023

27. Roberto Castro-Muñoz, Mohd Zamidi Ahmad, Magdalena Malankowska, Joaquín Coronas, A new relevant membrane application: CO2 direct air capture (DAC), Chemical Engineering Journal, Volume 446, Part 2, 2022, 137047, ISSN 1385-8947, https://doi.org/10.1016/j.cej.2022.137047

28. Lingcong Li, Shinta Miyazaki, Ziyang Wu, Takashi Toyao, Roman Selyanchyn, Zen Maeno, Shigenori Fujikawa, Ken-ichi Shimizu, Continuous direct air capture and methanation using combined system of membrane-based CO2 capture and Ni-Ca based dual functional materials, Applied Catalysis B: Environmental, Volume 339, 2023, 123151, ISSN 0926-3373, https://doi.org/10.1016/j.apcatb.2023.123151

29. May-Yin (Ashlyn) Low, Lucy Victoria Barton, Ronny Pini, Camille Petit, Analytical review of the current state of knowledge of adsorption materials and processes for direct air capture, Chemical Engineering Research and Design, Volume 189, 2023, Pages 745-767, ISSN 0263-8762, https://doi.org/10.1016/j.cherd.2022.11.040

30. Habib Azarabadi, Klaus S. Lackner, A sorbent-focused techno-economic analysis of direct air capture, Applied Energy, Volume 250, 2019, Pages 959-975, ISSN 0306-2619, https://doi.org/10.1016/j.apenergy.2019.04.012

31. Shi, X., Xiao, H., Azarabadi, H., Song, J., Wu, X., Chen, X., & Lackner, K. S. (2020). Sorbents for the direct capture of CO2 from Ambient Air. Angewandte

Chemie International Edition, 59(18), 6984–7006. https://doi.org/10.1002/anie.201906756

32. Sanz-Pérez, E. S., Murdock, C. R., Didas, S. A., & Jones, C. W. (2016). Direct capture of CO2 from Ambient Air. Chemical Reviews, 116(19), 11840–11876. https://doi.org/10.1021/acs.chemrev.6b00173

33. Mihrimah Ozkan, Saswat Priyadarshi Nayak, Anthony D. Ruiz, Wenmei Jiang, Current status and pillars of direct air capture technologies, iScience, Volume 25, Issue 4, 2022, 103990, ISSN 2589-0042, https://doi.org/10.1016/j.isci.2022.103990

34. IEA (2022), Direct Air Capture: A key technology for net zero, OECD Publishing, Paris, https://doi.org/10.1787/bbd20707-en.

35. Wiegner, J. F., Grimm, A., Weimann, L., & Gazzani, M. (2022). Optimal design and operation of solid sorbent direct air capture processes at varying ambient conditions. *Industrial & Engineering Chemistry Research*, *61*(34), 12649–12667. https://doi.org/10.1021/acs.iecr.2c00681

36. Leonzio, Grazia, Paul S. Fennell, and Nilay Shah. "Modelling and analysis of direct air capture systems in different locations." Chemical Engineering Transactions 96 (2022): 1-6.

37. Lackner, K. S., & Azarabadi, H. (2021). Buying down the cost of Direct Air Capture. Industrial & Engineering Chemistry Research, 60(22), 8196–8208. https://doi.org/10.1021/acs.iecr.0c04839

38. Patel, K.M. (2023). Application of Digital Twin for Direct Air Capture. CNCE Working Paper No. 0003, January 2023. Arizona State University KEEP Repository, https://hdl.handle.net/2286/R.2.N.183366

39. John Young, Fergus Mcilwaine, Berend Smit, Susana Garcia, Mijndert van der Spek, Process-informed adsorbent design guidelines for direct air capture, Chemical Engineering Journal, Volume 456, 2023, 141035, ISSN 1385-8947, https://doi.org/10.1016/j.cej.2022.141035

40. McLean, K. A., & McAuley, K. B. (2011). Mathematical modelling of Chemical Processes-obtaining the best model predictions and parameter estimates using identifiability and estimability procedures. The Canadian Journal of Chemical Engineering, 90(2), 351–366. https://doi.org/10.1002/cjce.20660

41. Jere Elfving, Cyril Bajamundi, Juho Kauppinen, Tuomo Sainio, Modelling of equilibrium working capacity of PSA, TSA and TVSA processes for CO2

adsorption under direct air capture conditions, Journal of CO2 Utilization, Volume 22, 2017, Pages 270-277, ISSN 2212-9820, https://doi.org/10.1016/j.jcou.2017.10.010

42. Dana Marinič, Blaž Likozar, Direct air capture multiscale modelling: From capture material optimization to process simulations, Journal of Cleaner Production, Volume 408, 2023, 137185, ISSN 0959-6526, https://doi.org/10.1016/j.jclepro.2023.137185

43. So-mang Kim, Grégoire Léonard, Process modelling of Direct Air Capture (DAC) of CO2 using solid amine sorbents, Editor(s): Ludovic outstruck, Stephane Negny, Computer Aided Chemical Engineering, Elsevier, Volume 51, 2022, Pages 265-270, ISSN 1570-7946, ISBN 780323958790, https://doi.org/10.1016/B978-0-323-95879-0.50045-X

44. Wiegner, J. F., Grimm, A., Weimann, L., & Gazzani, M. (2022). Optimal design and operation of solid sorbent direct air capture processes at varying ambient conditions. Industrial & Engineering Chemistry Research, 61(34), 12649–12667. https://doi.org/10.1021/acs.iecr.2c00681

45. Bender, Jamie. "Modelling for Sorbent Based Direct Air Capture Systems." (2023).

46. Sutherland, William. "LII. The viscosity of gases and molecular force." The London, Edinburgh, and Dublin Philosophical Magazine and Journal of Science 36, no. 223 (1893): 507-531. https://doi.org/10.1080/14786449308620508

47. Gilliland, Edwin Richard, and To K. Sherwood. "Diffusion of vapors into air streams." Industrial & Engineering Chemistry 26, no. 5 (1934): 516-523. https://doi.org/10.1021/ie50293a010

48. Satterfield, Charles N. "Mass transfer in heterogeneous catalysis." (1970).

49. Suzuki, Motoyuki, and M. Suzuki. Adsorption engineering. Vol. 14. Tokyo: Kodansha, 1990.

50. Perry's Chemical Engineers' Handbook. New York: McGraw-Hill, 1984.

51. Weather Spark. “The Weather Year-Round Anywhere on Earth - Weather Spark,” n.d. https://weatherspark.com/

52. “Carbon Removal Knowledge Gaps,” n.d. https://gaps.frontierclimate.com

APPENDIX A

PYTHON CODE: GENERALIZED PROCESS MODEL FOR SOLID SORBENT DIRECT AIR CAPTURE CONTACTORS

```
#Taking input from an Excel file

# import pandas library as pd
import pandas as pd
import math

# read excel file (here copy file path-text by right-clicking on the file path in explorer)
input_data = pd.read_excel("FILE-PATH")
print(input_data)

# Converting Excel data into required input for model calculation (STEP 1)

T = input_data.loc[0]['Value']
P = input_data.loc[1]['Value']
v = input_data.loc[2]['Value']
C_CO2 = input_data.loc[3]['Value']
L = input_data.loc[4]['Value']
W = input_data.loc[5]['Value']
S = input_data.loc[6]['Value']
H = input_data.loc[7]['Value']
sorbent_density = input_data.loc[9]['Value']
bed_porosity = input_data.loc[10]['Value']
particle_porosity = input_data.loc[11]['Value']
d_particle = input_data.loc[12]['Value']
Isotherm = input_data.loc[13]['Value']
d_pore = input_data.loc[14]['Value']
T_regen = input_data.loc[15]['Value']
pCO2_regen_inP = input_data.loc[16]['Value']
```

```
# Important process parameter calculation (STEP-2)
Mw_air = 28.96 #g/mol (molar mass of air)
Mw_CO2 = 44 #g/mol (molar mass of CO2)
D_CO2 = 0.000016 #m2/s (Diffusivity of CO2 in air)
R = 8.314 #J/mol K (Universal gas constant)

# Density of air calculation
rho_air = P*Mw_air/1000/(R*T) #kg/m3 (Density of air)
#print(rho_air)

# Sutherland's law constants for viscosity calculation
# These constants are specifically for air
C1 = 0.000001458
C2 = 110.4 #K

mu_air = C1*pow(T,1.5)/(T + C2) #Pa s (Viscosity of air)
#print(mu_air)

# Sorbent bed density calculation
bed_density = sorbent_density*(1-particle_porosity)*(1-bed_porosity) #kg/m3 (Sorbent bed
density considering particle and bed porosity)
#print(bed_density)

# equivalent diameter calculation for the channel
d_eq = 4*W*H/2*W #m (WH/2W is hydraulic radius)
#print(d_eq)
```

```
# Mass transfer coefficient calculations (STEP 3)

import numpy

# Reynolds number calculation
N_Re = d_eq*v*rho_air/mu_air #Reynold's number with equivalent diameter consideration
#print(N_Re)

#Alert for Laminar flow condition
if N_Re < 4000:
    alert_N_Re = "Flow is laminar. The geometry needs adjustment"
    print(alert_N_Re)
else:
    alert_N_Re = ''
    print(alert_N_Re)

# Schmidt number
N_Sc = mu_air/rho_air/D_CO2
#print(N_Sc)

# Interphase mass transfer calculation

# Sherwood number
Sh = 0.023*pow(N_Re,0.83)*pow(N_Sc,0.44)
#print(Sh)

# Interphase mass transfer coefficient
k_interphase = 2*Sh*D_CO2/d_eq #m/s
```

```
#print(k_interphase)

# Bed mass transfer calculation

# Interparticle mass transfer coefficient
D_bed = pow(bed_porosity,2)*D_CO2 #m2/s
#print(D_bed)

# Particle mass transfer coefficient

# Mean free path calculation
l = 3.2*mu_air/P*pow((R*T*1000/(2*numpy.pi*Mw_CO2)),0.5) #m
#print(l)

# Knudsen number
Kn = d_pore/l
#print(Kn)

# Knudsen diffusion coefficient
Dk = 48.5*d_pore*pow((T/Mw_CO2*1000),0.5) #m2/s
#print(Dk)

if Kn >= 10: #Coventional diffusion will be dominate
   D_particle = pow(particle_porosity,2)*D_CO2
   print("Conventional diffusion in the particle")
   #print(D_particle)

elif Kn <= 0.1: #Knudsen diffusion will dominate
```

```
    D_particle = pow(particle_porosity,2)*Dk
    print("Knudsen diffusion in the particle")
     #print(D_particle)

elif 0.1<Kn<10: #Both diffusion will be equally important
        De = 1/((1/D_CO2) + (1/Dk))
        D_particle = pow(particle_porosity,2)*De
        print("Mixed diffusion in the particle")
        #print(D_particle)

# Overall mass transfer coefficient calculation
k = 1/((1/k_interphase) + (S/2/D_bed) + (d_particle/2/D_particle)) #(m/s)
#print(k)



# Mass balance and model run (STEP 4)
F_air = v*H*W #m3/s (Flow of air)
Number_of_unit_cells = L/0.001 #(Defining numbers of the unit cell) Also this can be adjusted for changing precision.
C_CO2_IN_Master = C_CO2 #ppm
unit_cell_sorbent_mass = 0.001*0.01*S/2*bed_density*1000 #g Calculation mass of sorbent in each unit cell


#print(unit_cell_sorbent_mass)


#Toth Isotherm parameters
qsat1_start = 2.6 #mmol/g
b1_start = 8.2045*10**-15*math.exp(82362.5/T_regen/8.314) #mbar-1  This is solved using Van't Hoff correlation externally
```

```
#print(b1)

b2_start = 5.4441/(10**8)*math.exp(25542.8/T_regen/8.314) #mmol/g mbar This is solved using Van't Hoff correlation externally

#print(b2)



#Toth Isotherm parameters

qsat1 = 2.6 #mmol/g

b1 = 8.2045*10**-15*math.exp(82362.5/T/8.314) #mbar-1  This is solved using Van't Hoff correlation externally

#print(b1)

b2 = 5.4441/(10**8)*math.exp(25542.8/T/8.314) #mmol/g mbar This is solved using Van't Hoff correlation externally

#print(b2)


#Nested lists for process OUTPUTS


#CO2 loading rate list

CO2_loading_rate_list = []


#Output CO2 concentration list

C_CO2_OUT_list = []


#Equilibrium CO2 concentration list for each cell

Q_CO2_eq_list = []


#Total CO2 loading list for each time instance for each cell

Q_CO2_list= [[]]
```

```
#Master loop condition calculation

#Partial pressure conversion from ppm to mbar
pCO2 = C_CO2_IN_Master*P/pow(10,8)

# Equilibrium CO2 loading calculation
Q_CO2_eq_master = qsat1*b1*pCO2/(1+(b1*pCO2)) + b2*pCO2
print("Final Loading = " + str(Q_CO2_eq_master) + "mmol/g")



#This is to calculate the starting condition based on the regeneration temperature
pCO2_regen = pCO2_regen_inP/100  #mbar
#print(pCO2_regen)
Q_CO2_start = qsat1_start*b1_start*pCO2_regen/(1+(b1_start*pCO2_regen)) +
b2_start*pCO2_regen
print("Initial Loading = " + str(Q_CO2_start) + "mmol/g")

#Creating a list for External While LOOP condition
Q_CO2_eq_master_list = [Q_CO2_eq_master]*int(Number_of_unit_cells)
#print(Q_CO2_eq_master_list)

#Creating the first list with ZERO loading based on obtained numbers of the unit cell
j = 0
while j < Number_of_unit_cells:
    Q_CO2_list[0].append(Q_CO2_start)
    j = j+1
```

```
#print(Q_CO2_list)

#List for while LOOP condition
condition_list = [i * 0.999 for i in Q_CO2_eq_master_list ]
#print(conditional_list)

#Time list
time_list = []
t = 1

#External while LOOP for the equilibrium calculation
while Q_CO2_list[t-1][-1] < condition_list[-1]:

    #Tester codes
    #print(C_CO2_IN)
    #print(Q_CO2_list[t-1])

#Use this LOOP for time-limiting calculation (may come in handy for cycle-time testing and rating studies)
#while t < 5:

    #Model run for a particular time instance

    #Lists to collect OUTPUT for that particular time instant 't'

    #CO2 loading rate at time 't'
    CO2_loading_rate_list_t = []

    #Outlet CO2 concentration at a time 't'
```

```
C_CO2_OUT_list_t = []

#Total CO2 loading for that particular time instant 't'
Q_CO2_list_t = []

#Inlet CO2 concentration for the first unit cell (as per defined CO2 concentration in the inlet)
C_CO2_IN = C_CO2 #ppm (inlet CO2 concentration)



#Tester codes
#print(Q_CO2_list_t)
#print(Q_CO2_list[t-1])

i = 0

#Internal while LOOP for unit cell transition (STEP 5)
while i < Number_of_unit_cells:

    #Tester codes
    #print(C_CO2_IN)
    #print(C_CO2_IN)

    #Toth isotherm equation
    pCO2 = C_CO2_IN*P/pow(10,8) #Unit conversion ppm to Pa
    #print(pCO2)

    #Equilibrium concentration based on inlet CO2 concentration for the unit cell
    Q_CO2_eq = qsat1*b1*pCO2/(1+(b1*pCO2)) + b2*pCO2
```

```
            #print(Q_CO2_eq)
            Q_CO2_eq_list.append(Q_CO2_eq)

            #Mass balance equation
            # (CO2 flow IN) - (CO2 flow OUT) = Rate of accumulation
            #print(Q_CO2_list[t-1][i])

            #CO2 loading rate calculation equation
            CO2_loading_rate = bed_density*k*(Q_CO2_eq - Q_CO2_list[t-1][i])/10
#mmol/cm2s where 1000 is unit conversion factor
            #print(CO2_loading_rate)
            CO2_loading_rate_list_t.append(CO2_loading_rate)

            #Outlet CO2 concentration
            C_CO2_OUT = C_CO2_IN - pow(10,6)*0.1*CO2_loading_rate*pow(10,-
            3)/(v*H*P*0.01/(2*R*T))
            #ppm (The 0.01 is for unit cell dimension-width)

            #print(C_CO2_OUT)
            C_CO2_OUT_list_t.append(C_CO2_OUT)
            C_CO2_IN = C_CO2_OUT
            i = i+1

    #Tester codes
    #print(C_CO2_OUT_list_t)
    #print(Q_CO2_eq_list)
    #print(CO2_loading_rate_list_t, len(CO2_loading_rate_list_t))
    #print(len(CO2_loading_rate_list_t))
    #print(Q_CO2_list[t])
```

```
    #Calculating cumulative loading of the cell
    z = 0
    for z in range(0, len(CO2_loading_rate_list_t)):
        #print(z, len(Q_CO2_list[t-1]))
        Q_CO2_list_t.append(Q_CO2_list[t-1][z] + CO2_loading_rate_list_t[z])



    #print(Q_CO2_list_t, len(Q_CO2_list_t))



    #Nested list appending
    CO2_loading_rate_list.append(CO2_loading_rate_list_t)
    C_CO2_OUT_list.append(C_CO2_OUT_list_t)
    Q_CO2_eq_list.append(Q_CO2_eq_list)
    Q_CO2_list.append(Q_CO2_list_t)
    #print(t)

    time_list.append(t)
    t = t+1

#Tester codes

#List printer
#print(CO2_loading_rate_list_t)
#print(Q_CO2_list_t)
#print(C_CO2_OUT_list_t)
#print(Q_CO2_eq_list_t)
```

```
#print(time_list)
#print(Q_CO2_list_t2)



#Nested list printer
#print(CO2_loading_rate_list)
#print(Q_CO2_list)
#print(C_CO2_OUT_list)
#print(Q_CO2_eq_list)

#Converting the OUPUT nested list to the data frame

# import pandas as pd
import pandas as pd

# Calling DataFrame constructor on the list
CO2_loading_data = pd.DataFrame(Q_CO2_list)
CO2_loading_rate_data = pd.DataFrame(CO2_loading_rate_list)
CO2_outlet_concentration_data = pd.DataFrame(C_CO2_OUT_list)

#Dropping first one to make a consistent size data frame
CO2_loading_data = CO2_loading_data.drop(0)

#print(CO2_loading_rate_data)
#print(CO2_outlet_concentration_data)
#print(CO2_loading_data)

#Here axis  = 0 will do the sum vertically while 1 will do this horizontally
```

```
cumulative_loading_data = CO2_loading_data.sum (axis = 1) #This is for one strip
#print(cumulative_loading_data)
#print(cumulative_loading_data_bed)



#Output results
print("\nReynolds number:" + str(N_Re))
print("Schmidt number:" + str(N_Sc))
print("Sherwood number:" + str(Sh))
print("Interphase mass transfer coefficient:" + str(k_interphase) + "m/s")
print("Diffusion coefficient of CO2 in the bed:" + str(D_bed) + "m2/s")
print("Kundsen number:" + str(Kn))
print("Overall mass transfer coefficient:" + str(k) + "m/s")
print("Total loading time for the bed:" + str(time_list[-1]) + "s")
print("Volumetric flowrate:" + str(F_air) + "m3/s")
```

#Unit Cell Loading Curve

```
import matplotlib.pyplot as plt
import numpy as np

#Function for generating sub-plots
fig, (ax1, ax3) = plt.subplots(2, figsize=(6,8))
#In this bracket type (x,y) where x gives no. of graphs vertically and y gives no. graph horizontally
#figsize (x,y): x - width, y - height

fig.suptitle('CO2 loading curves', fontweight = 'bold', size = 16)

y = {} #Created dictionary to individual curves for each unit cell
x = time_list

ax1.set_title('Unit cell loading')
ax3.set_title('Unit cell loading in mmol of CO2')

ax1.set(xlabel='Time (s)', ylabel='CO2 loading (mmol/g)')
ax3.set(xlabel='Time (s)', ylabel='CO2 loading (mmol)')

#Unit Cell loading curve generation
o = 0
while o < Number_of_unit_cells:
    y[o] = CO2_loading_data[o]
    ax1.plot(x, y[o])
    o += 1

#Cell loading in  mmol of CO2
```

```
CO2_loading_data2 = CO2_loading_data.multiply(unit_cell_sorbent_mass)
#print(CO2_loading_data2)
total_strip_loading = CO2_loading_data2.sum(axis=1)
total_bed_loading = total_strip_loading.mul(W*100*2)
#print(total_bed_loading)

#Channel capacity determination
#print(total_bed_loading.iloc[1])
#print(total_bed_loading.iloc[-1])
channel_capacity = (total_bed_loading.iloc[-1] - total_bed_loading.iloc[1])/1000
print("Channel Capacity(mol): " +  str(channel_capacity))

y1 = {} #Created dictionary to individual curves for each unit cell
#Total CO2 cell loading curve
o = 0
while o < Number_of_unit_cells:
    y1[o] = CO2_loading_data2[o]
    ax3.plot(x, y1[o])
    o += 1

# Set the spacing between subplots
fig.tight_layout()
# tight_layout() method automatically maintains the proper space between subplots
```

#Cumulative loading curve (*STEP 6*)

```
import matplotlib.pyplot as plt

import numpy as np


fig, (ax2) = plt.subplots(1, figsize=(6,4))

#In this bracket type (x,y) where x gives no. of graphs vertically and y gives no. graph horizontally

#figsize (x,y): x - width, y - height


#Setting up chart title and axis labels

ax2.set_title('Total channel loading data', fontsize = 16)

#ax2.set(xlabel='Time (s)', ylabel='Average CO2 loading rate(mmol/cm2s)')

plt.xlabel('Time (s)', fontsize = 14)

plt.ylabel('CO2 loading (mmol)', fontsize = 14)


x = time_list


ax2.plot(x,total_bed_loading)

fig.tight_layout()


#saving graph in PNG

plt.savefig(r'FILEPATH')
```

#Average Loading Rate Curve

```
import matplotlib.pyplot as plt

import numpy as np


fig, (ax4) = plt.subplots(1, figsize=(6,4))

#In this bracket type (x,y) where x gives no. of graphs vertically and y gives no. graph horizontally

#figsize (x,y): x - width, y - height


ax4.set_title('Average loading rate curve', fontsize = 16)

#ax4.set(xlabel='Time (s)', ylabel='CO2 loading (mmol/g)')

plt.xlabel('Time (s)', fontsize = 14)

plt.ylabel('CO2 loading rate (mmol/mm2s)', fontsize = 14)


x = time_list


Avg_CO2_loading_rate = CO2_loading_rate_data.mean(axis = 1) # for row avg. axis = 1 while axis = 0 for column average


ax4.plot(x, Avg_CO2_loading_rate)


fig.tight_layout()


plt.savefig(r'FILEPATH')
```

#CSV file generation

```
#loading_data_array = CO2_loading_data[0].tolist()
#print(loading_data_array)
#print(time_list)
i = 0
unit_cell_no = []
while i < time_list[-1]:
    unit_cell_no.append(1)
    i += 1
#print(unit_cell_no)
#print(CO2_loading_data)
#print(CO2_loading_data[1][1])

# Dataframe with defined column headers

i = 0
column = []
while i < Number_of_unit_cells:
    column.append("Unit Cell No " + str(i+1))
    i += 1

#print(column)

column2 = column
column3 = column

CO2_loading_data.columns = column
CO2_outlet_concentration_data.columns = column2
```

```
CO2_loading_rate_data.columns = column3

#print(CO2_loading_data)          #This will require reduction of 1st row due to initial zero row.
#print(CO2_loading_rate_data)
#print(CO2_outlet_concentration_data)

#Dataframe to CSV file creation on the local server
#This file can be downloaded as required

CO2_loading_data.to_csv(r"FILEPATH")
CO2_outlet_concentration_data.to_csv(r" FILEPATH ")
CO2_loading_rate_data.to_csv(r" FILEPATH ")
total_bed_loading.to_csv(r" FILEPATH ")
Avg_CO2_loading_rate.to_csv(r" FILEPATH ")
```

#Output Report table creation

```
import pandas as pd
from datetime import date

case_date = date.today()
#print(case_date)

#table 1
Result_table = {1:['Case No.','Date','Contactor type','Type of Adsorbent','CHANNEL
PROPERTIES','Channel Velocity (m/s)','Bed void fraction',
        'Particle porosity','Material density (kg/m3)','Bulk Density (kg/m3)','Average pore
diameter (m)',
        'AMBIENT CONDITIONS','Temperature (K)','Pressure (Pa)','CO2 concentration
(ppm)',
        'SORBENT PROPERTIES','Isotherm','Equilibrium loading time (s)'],
       2:['001', case_date, 'Parallel plate', 'MIL 101 (Cr)','', v , bed_porosity, particle_porosity,
        sorbent_density, bed_density, d_pore, '', T, P, C_CO2, '','Toth', time_list[-1] ]}

Result_table1 = pd.DataFrame(Result_table)
Result_list = Result_table1.values.tolist()

#print(Result_list)
#table 2
MT_table = {1:['Parameter','Reynolds No.','Schmidt No.','Sherwood No.','Interphase MT
coefficient (m/s)',
        'Interparticle MT coefficient (m/s)','Intraparticle MT coefficient (m/s)','Overall MT
coefficient (m/s)',
        'Initial sorbent loading (mmol/g)','Equilibrium sorbent loading (mmol/g)',
"Regeneration temperature (K)",
        "CO2 partial pressure (Pa)", "Channel Capacity (net)(mol)"],
```

```
        2:['Unit',round(N_Re, 4), round(N_Sc, 4), round(Sh, 4), round(k_interphase,8),
round(D_bed, 9), round(D_particle, 9),

          round(k, 8), round(Q_CO2_start,4), round(Q_CO2_eq_master,4), str(T_regen),
str(pCO2_regen*100), round(channel_capacity,4)]}


MT_table1 = pd.DataFrame(MT_table)

MT_list = MT_table1.values.tolist()


print(MT_list)


alert_table = {1:['ALERTS', alert_N_Re]}

alert_table1 = pd.DataFrame(alert_table)

alert_list = alert_table1.values.tolist()

print(alert_list)


import pandas as pd


#Dataframe to list conversion for ease of coding

df1 = total_bed_loading.values.tolist()

df2 = Avg_CO2_loading_rate.values.tolist()

df3 = CO2_outlet_concentration_data[CO2_outlet_concentration_data.columns[-1]]

df3 = df3.values.tolist()

#print(df3)


#List created for master table

table1 = {'time(s)': time_list, 'Total bed loading (mmol/cm2)': df1, 'Average loading rate
(mmol/cm2s)': df2, 'Outlet CO2 concentration (ppm)': df3}


#Converted list data to data frame master table
```

```
df4 = pd.DataFrame(table1)



#Closest value result which will be compared and retrieved
value1 = 0.25*df1[-1]
value2 = 0.5*df1[-1]
value3 = 0.75*df1[-1]
value4 = 0.9*df1[-1]
#Looks for a specific value in the column and returns the whole row
#df3.loc[df3['Total bed loading (mmol/cm2)'] == value1]

#Looks for values close to the given conditional values
r1 = df4.iloc[(df4['Total bed loading (mmol/cm2)']-value1).abs().argsort()[:1]]
r2 = df4.iloc[(df4['Total bed loading (mmol/cm2)']-value2).abs().argsort()[:1]]
r3 = df4.iloc[(df4['Total bed loading (mmol/cm2)']-value3).abs().argsort()[:1]]
r4 = df4.iloc[(df4['Total bed loading (mmol/cm2)']-value4).abs().argsort()[:1]]

#print(r1)
#print(r2)
#print(r3)
#print(r4)

r11 = r1.values.tolist()
r21 = r2.values.tolist()
r31 = r3.values.tolist()
r41 = r4.values.tolist()
#rint(r11)
```

```
Loading_table = {1:['% Net loading','Time (s)', 'Total CO2 loading (mmol)', 'Average loading rate (mmol/cm2s)',
                    'Outlet CO2 concentration (ppm)'],
                2: ['25%',r11[0][0], round(r11[0][1], 6), round(r11[0][2],6), round(r11[0][3], 3)],
                3: ['50%',r21[0][0], round(r21[0][1], 6), round(r21[0][2], 6), round(r21[0][3], 3)],
                4: ['75%',r31[0][0], round(r31[0][1], 6), round(r31[0][2], 6), round(r31[0][3], 3)],
                5: ['90%',r41[0][0], round(r41[0][1], 6), round(r41[0][2], 6), round(r31[0][3], 3)]}

#print(Loading_table)
Loading_table1 = pd.DataFrame(Loading_table)
Loading_list = Loading_table1.values.tolist()

#print(Loading_list)
```

#Breakthrough curve data

```
#print(CO2_outlet_concentration_data)
value5 = r11[0][0]
value6 = r21[0][0]
value7 = r31[0][0]
value8 = r41[0][0]
r5 = CO2_outlet_concentration_data.loc[value5]
r6 = CO2_outlet_concentration_data.loc[value6]
r7 = CO2_outlet_concentration_data.loc[value7]
r8 = CO2_outlet_concentration_data.loc[value8]

r51 = r5.values.tolist()
r61 = r6.values.tolist()
r71 = r7.values.tolist()
```

```
r81 = r8.values.tolist()


#print(r51)
#print(r61)


import matplotlib.pyplot as plt
import numpy as np


fig, (ax5) = plt.subplots(1, figsize=(6,4))
#In this bracket type (x,y) where x gives no. of graphs vertically and y gives no. graph horizontally
#figsize (x,y): x - width, y - height


#Labelling Chart
ax5.set_title('Breakthrough curve', fontsize = 16)
#ax5.set(xlabel='Length (cm)', ylabel='CO2 Outlet concentration (ppm)')


plt.xlabel('Length (mm)', fontsize = 14)
plt.ylabel('CO2 Outlet concentration (ppm)', fontsize = 14)


i1 = 1
x = []
while i1 <= Number_of_unit_cells:
    x.append(i1)
    i1= i1+1


#Graph generation
ax5.plot(x, r51)
ax5.plot(x, r61)
```

```
ax5.plot(x, r71)
ax5.plot(x, r81)

#plt.annotate('25%', xy=(x[-5], r51[-5]))
#plt.annotate('50%', xy=(x[5], r61[5]))
#plt.annotate('75%', xy=(x[7], r71[7]))
#plt.annotate('90%', xy=(x[-2], r81[-2]))

ax5.legend(['25%','50%','75%', '90%'])
fig.tight_layout()
#saving graph in PNG
plt.savefig(r' FILEPATH ')
```

#Report Creation on Canvas in the form of PDF (*STEP 7*)

```
from reportlab.lib.pagesizes import letter,A4
from reportlab.lib import colors
from reportlab.lib.units import inch
from reportlab.pdfgen import canvas
from reportlab.platypus import Table, Paragraph, Image

# Create a canvas with a specified page size
c = canvas.Canvas(r" FILEPATH", pagesize=A4)

# Define table styles
table_style = [
    ('BACKGROUND', (0, 0), (-1, 0), colors.white),
    ('TEXTCOLOR', (0, 0), (-1, 0), colors.black),
    ('ALIGN', (0, 0), (-1, -1), 'LEFT'),
    ('FONTNAME', (0, 0), (-1, 0), 'Helvetica-Bold'),
    ('FONTSIZE', (0, 0), (-1, 0), 12),
    ('BOTTOMPADDING', (0, 0), (-1, 0), 12),
    ('BACKGROUND', (0, 1), (-1, -1), colors.white),
    ('GRID', (0, 0), (-1, -1), 1, colors.black),
]

# Define sample text
text = "Process Modelling Results Sheet for Direct Air Capture Contactor"
length = "Length = " + str(L) + "m"
width  = "Width = " + str(W) + "m"
thickness  = "Height = " + str(S) + "m"
```

```
gap  = "Gap = " + str(H) + "m"
FigureTitle = "Geometry of the bed"

# Draw the table on the canvas
table = Table(Result_list)
table.setStyle(table_style)
table.wrapOn(c, 0.5*inch, 10*inch)
table.drawOn(c, 0.5*inch, 6.4*inch)

# Draw the table on the canvas
table = Table(MT_list)
table.setStyle(table_style)
table.wrapOn(c, 3.5*inch, 4.5*inch)
table.drawOn(c, 0.5*inch, 2.9*inch)

# Draw the table on the canvas
table = Table(alert_list)
table.setStyle(table_style)
table.wrapOn(c, 400, 20)
table.drawOn(c, 0.5*inch, 1.7*inch)

# Draw the table on the canvas
table = Table(Loading_list)
table.setStyle(table_style)
table.wrapOn(c, 400, 20)
table.drawOn(c, 0.5*inch, 0.15*inch)
```

```
# Set the font and font size for the canvas
c.setFont("Helvetica-Bold", 13.5)
# Draw the text on the canvas
c.drawString(0.15*inch, 11.3*inch, text)



# Draw the image on the canvas
c.drawImage('LOGO FILEPATH', 6.1*inch, 10.95*inch, width=2.2* inch, height=0.75 *
inch)

# Draw the image on the canvas
c.drawImage('IMAGE FILEPATH', 4.2*inch, 8.2*inch, width=3* inch, height=2.5 *
inch)

# Set the font and font size for the canvas
c.setFont("Helvetica", 10)
# Draw the text on the canvas
c.drawString(7*inch, 9.5*inch, length)
c.drawString(5.8*inch, 10.5*inch, width)
c.drawString(3.6*inch, 9.67*inch, thickness)
c.drawString(3.7*inch, 9.47*inch, gap)

# Set the font and font size for the canvas
c.setFont("Helvetica-Bold", 12)
# Draw the text on the canvas
c.drawString(5.5*inch, 10.7*inch, FigureTitle)

# Draw the average loading rate curve on the canvas
```

```
c.drawImage(r'Average loading rate curve FILEPATH', 4*inch, 5.8*inch, width=3.7*
inch, height=2.1 * inch)


# Draw the cumulative loading curve on the canvas

c.drawImage(r' Cumulative loading curve FILEPATH ', 4.2*inch, 3.7*inch, width=3.5*
inch, height=2.1 * inch)


# Draw the breakthrough curve on the canvas

c.drawImage(r' Breakthrough curve FILEPATH', 4.2*inch, 1.55*inch, width=3.5* inch,
height=2.1 * inch)

# Save the canvas as a PDF file

c.save()
```

APPENDIX B

SAMPLE DESIGN RESULT REPORT

Process Modelling Results Sheet for Direct Air Capture Contactor

Center for Negative Carbon Emissions
Arizona State University

Case No.	001
Date	2023-09-27
Contactor type	Parallel plate
Type of Adsorbent	MIL 101 (Cr)
CHANNEL PROPERTIES	
Channel Velocity (m/s)	2
Bed void fraction	0.4
Particle porosity	0.4
Material density (kg/m3)	1000
Bulk Density (kg/m3)	360.0
Average pore diameter (m)	1e-09
AMBIENT CONDITIONS	
Temperature (K)	298
Pressure (Pa)	98000
CO2 concentration (ppm)	420
SORBENT PROPERTIES	
Isotherm	Toth
Equilibrium loading time (s)	5724

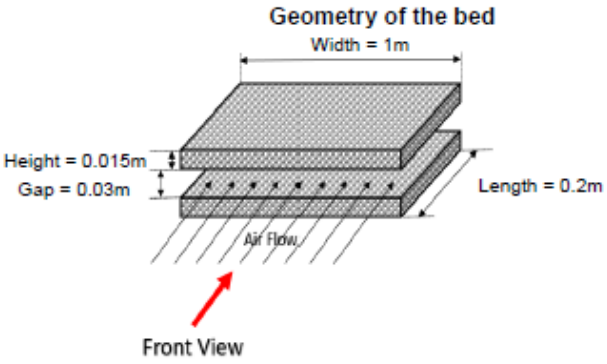

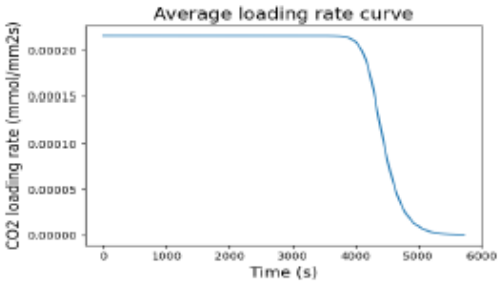

Parameter	Unit
Reynolds No.	7484.8553
Schimdt No.	1.002
Sherwood No.	37.8169
Interphase MT coefficient (m/s)	0.02016903
Interparticle MT coefficient (m/s)	2.56e-06
Intraparticle MT coefficient (m/s)	6.39e-07
Overall MT coefficient (m/s)	0.00029667
Initial sorbent loading (mmol/g)	0.2873
Equilibrium sorbent loading (mmol/g)	1.2496
Regeneration temperature (K)	368
CO2 partial pressure (Pa)	3000.0
Channel Capacity (net)(mol)	1.0388

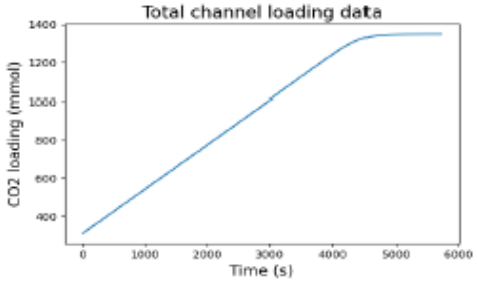

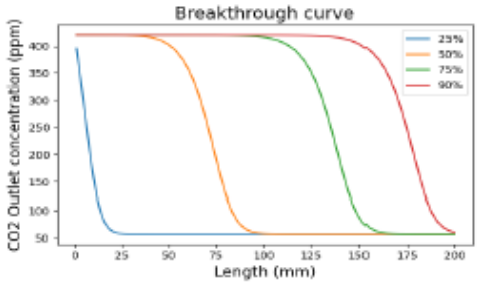

ALERTS

% Net loading	25%	50%	75%	90%
Time (s)	117.0	1565.0	3013.0	3883.0
Total CO2 loading (mmol)	337.495263	674.85647	1012.217641	1214.669546
Average loading rate (mmol/cm2s)	0.000216	0.000216	0.000216	0.000214
Outlet CO2 concentration (ppm)	56.41	56.41	56.411	56.411